

# Shaken, not stirred—or rather phase-separated? Photophysics of pentacene-based binary blends and the relevance of local structure

Cite as: Chem. Phys. Rev. **7**, 021307 (2026); doi: [10.1063/5.0295855](https://doi.org/10.1063/5.0295855)

Submitted: 11 August 2025 · Accepted: 28 April 2026 ·

Published Online: 13 May 2026



View Online



Export Citation



CrossMark

Frederik Unger and Frank Schreiber<sup>a)</sup>

## AFFILIATIONS

Institute of Applied Physics, University of Tübingen, Auf der Morgenstelle 10, 72076 Tübingen, Germany

<sup>a)</sup>Author to whom correspondence should be addressed: [frank.schreiber@uni-tuebingen.de](mailto:frank.schreiber@uni-tuebingen.de)

## ABSTRACT

The electronic and optical properties of organic semiconductors are strongly determined by their structural properties. Combining two or more semiconductor compounds in multicomponent blends is commonly exploited to tune the properties and meet the requirements for high-performance applications such as organic solar cells, light-emitting diodes, and transistors. Here, we discuss the structural and optical properties characteristic of binary systems containing the archetypal organic semiconductor pentacene. Typical examples are shown for the formation of a solid solution, a co-crystal, and phase separation. They not only allow the elucidation of the mixing behavior in more complicated binary systems but also broaden the understanding of binary blends in general. We highlight the importance of the local occupation configuration geometry and environment beyond the global thermodynamic mean-field considerations of mixing vs demixing. A thorough understanding of mixing in small organic molecule binary blends on the nanoscale is highly beneficial for capitalizing on the full power of organic semiconductors.

Published under an exclusive license by AIP Publishing. <https://doi.org/10.1063/5.0295855>

## TABLE OF CONTENTS

|  |    |
|--|----|
| I. INTRODUCTION                                      | 1  |
| II. THERMODYNAMIC CONSIDERATIONS FOR BINARY MIXTURES |    |
| A. The regular solution model                        | 3  |
| B. Mixing scenarios                                  | 4  |
| C. Beyond regular solution theory                    | 4  |
| III. PRISTINE PEN                                    | 5  |
| A. Structural properties                             | 5  |
| B. Optical properties                                | 5  |
| C. Growth mode and molecular dimensions              | 6  |
| IV. SOLID SOLUTION                                   | 6  |
| A. Structural properties                             | 7  |
| B. Optical properties                                | 8  |
| C. Conclusion  | 9  |
| V. PHASE-SEPARATING SYSTEMS                          | 9  |
| A. Structural properties                             | 9  |
| B. Optical properties                                | 10 |
| VI. CO-CRYSTAL FORMATION                             | 11 |
| A. Structural properties of equimolar blends         | 11 |
| B. Optical properties of equimolar blends            | 11 |
| C. Conclusion for equimolar blends                   | 11 |

|   |    |
|---|----|
| D. Phase separation in co-crystal blends    | 12 |
| VII. COMPLEX OR INTERMEDIATE MIXING REGIMES | 12 |
| A. Thickness-dependent mixing               | 12 |
| B. Partial phase separation                 | 14 |
| VIII. SUMMARY AND FUTURE DIRECTIONS         | 15 |

## I. INTRODUCTION

Understanding the structure–property relationship is central to the use of crystalline organic semiconductor blends in modern optical, electronic, and optoelectronic applications based on organic molecules. Since many of these devices are based on two or even more molecular compounds, it is crucial to have precise knowledge of and to be able to actively control the mixing behavior and, consequently, the electronic and optical properties.<sup>1</sup> Importantly, as different applications demand optimization of various properties, changing and controlling the mixing behavior is of particular interest.

As a typical example, in organic solar cells, the power conversion efficiency can be enhanced by maximizing the donor–acceptor interface area. While this improves the efficiency of charge separation, also the unperturbed, neat phases in their crystalline, well-ordered state

are required for efficient charge transport.<sup>2–4</sup> Thus, phase separation on the nanometer length scale, as realized, for example, in bulk heterojunction device architectures, is one strategy for improving power conversion efficiencies in organic solar cells.<sup>3–7</sup> In contrast, mixing on the molecular level has been shown to facilitate continuous tuning of optical, electronic, and viscoelastic properties.<sup>8–12</sup> This encompasses modification of color tones and optimization of photophysical properties through the selection of an appropriate mixing ratio.<sup>13,14</sup> Furthermore, the combination of two small organic molecule semiconductor compounds in a crystalline organic alloy has been shown to protect the device from degradation while maintaining high conductivity.<sup>15</sup> While in all of these cases, a continuous change of the given properties has been reported, it is also possible that the interaction between the different molecular compound entities results in distinct new properties. For example, new crystal structures may be formed.<sup>16</sup> In addition, the generation of charge-transfer states often leads to the observation of low-energy optical transitions.<sup>17</sup> Such a transfer of charges can be exploited in doping molecular binary mixtures to increase electrical conductivity.<sup>18,19</sup> A profound understanding of this classical doping mechanism in organic semiconductor compounds also helps for the development and improvement in the latest, sophisticated doping approaches.<sup>20</sup>

These general examples demonstrate the importance of precise knowledge of the mixing characteristics and associated structural and optical properties to capitalize on the full potential of a given organic semiconductor.<sup>21,22</sup> Additionally, the multicomponent organic structures compose the internal active layer of a device, which can be further optimized for its desired application using modern external design strategies.<sup>23</sup> Furthermore, it is important to note that not only the overall, macroscopic characterization in terms of mixing and demixing is sufficient, but also the meso- to nanoscopic structure and the local environment, such as the question of occupation configuration geometry, can be crucial since different functional properties couple to different length scales.<sup>24</sup> Thus, profound knowledge of the mixing behavior and its implication on properties, including optical absorption, is essential for an understanding of the structure–property relationship in organic binary mixtures.

In this paper, we discuss the various mixing scenarios and associated structural and optical signatures for the organic semiconductor pentacene [PEN, molecular structure shown in Fig. 1(b)] in combination with a variety of small organic molecule materials for the second compound. PEN serves as a prototypical small organic molecule, with the results presented here being transferable to other rod-like organic semiconductors such as tetracene [TET, Fig. 1(c)] and diindenoperylene [DIP, Fig. 1(c)] with some level of generality.<sup>24–26</sup> The interest in PEN and its role as a model compound for organic semiconductors originates from its high hole mobility<sup>27–31</sup> and its ability to undergo singlet exciton fission, the conversion of a singlet exciton into two triplet excitons.<sup>32–35</sup> The former property has been exploited by using PEN in thin-film transistors,<sup>29,36</sup> while the latter has stimulated additional interest in the application of PEN in organic solar cells. This is because the singlet exciton fission mechanism holds great promise for increasing the power conversion efficiency of solar cells beyond the Shockley–Queisser limit.<sup>37–41</sup> In addition, this capability for exciton multiplication can be exploited in PEN-based photodetectors.<sup>42</sup>

The PEN-based binary mixtures discussed in this paper serve as a benchmark for the full range of mixing scenarios encountered in small

molecule binary blends with crystalline order in general. These include the formation of occupationally disordered solid solutions, phase separation, and the formation of ordered co-crystals (Fig. 1). We focus on small organic molecule systems prone to crystalline order while amorphous systems are not included. We note that amorphous structures, as found in organic glasses, are of equal interest from both a fundamental and an applied perspective, as they are widely used, for example, in organic light-emitting diodes.<sup>43–45</sup> The restriction to polycrystalline, thin-film samples of similar thickness on flat, weakly interacting substrates further excludes thickness dependence of the structural and optical properties, epitaxy, azimuthal molecular alignment, and in-plane anisotropies from the discussion presented here.<sup>46–49</sup> Furthermore, while doping in organic semiconductors is typically done at low mixing ratios below 10% dopant concentration, here, focus is given to intermediate mixing ratios (see, e.g., Refs. 50 and 51 for reviews on doping in organic semiconductors). Nevertheless, it should be noted that doping at higher dopant concentrations has recently attracted increasing interest for application in the most efficient optoelectronic devices,<sup>51</sup> thus bridging the gap to the here investigated intermediate mixing ratios. Additionally, the efficiency of doping at both low and high mixing ratios is severely affected by the distribution of the dopant and the ordering on mesoscopic and nanoscopic length scales, highlighting the importance of the structure–property relationship in binary blends.<sup>51,52</sup> For example, aggregation of dopants instead of a nanoscopic homogeneous intermixing can be detrimental for doping efficiency.<sup>51</sup> Thus, a detailed understanding of the mixing scenarios encountered in organic binary systems, as discussed here, will also contribute to a better understanding of doping in organic semiconductors. In addition to x-ray diffraction measurements, optical absorption properties provide complementary information on the ordering at different length scales. The latter are further interesting for modern optoelectronic devices such as organic light-emitting diodes and organic solar cells but also can be of fundamental interest for the characterization of organic field-effect transistors and organic thermoelectrics.<sup>51</sup> Therefore, this investigation provides guidelines for the choice of the second molecular compound to optimize the optoelectronic properties of the organic semiconductor of interest. While we focus here on the characterization of small organic molecule binary blends using x-ray diffraction and optical absorption spectroscopy for consistency, complementary techniques exist, such as (photo-induced) atomic force microscopy, vibrational spectroscopy, and electron energy-loss spectroscopy, which can probe structural or optoelectronic properties across different length scales.<sup>53–57</sup>

This paper is organized as follows. First, the different types of mixing scenarios are introduced based on a mean-field approach. These general considerations are complemented by highlighting the importance of the mesoscopic structure. Next, the fundamental properties of neat PEN are summarized to understand the changes that occur in the binary mixtures. In the following three parts, the structural and optical absorption properties characteristic of solid solutions, phase separations, and systems forming co-crystals containing PEN are demonstrated using model binary systems. These samples were prepared by organic molecular beam deposition (OMBD), which allows for precise control of the mixing ratio (for details on the sample preparation see Refs. 13, 24, 25, and 58–68). We note that thin-film growth by OMBD is a non-equilibrium process that enables sample preparation with mixing ratios beyond the thermodynamic solubility limit.<sup>69,70</sup> For the structural properties, x-ray diffraction techniques were employed. Depending on the mixing behavior,

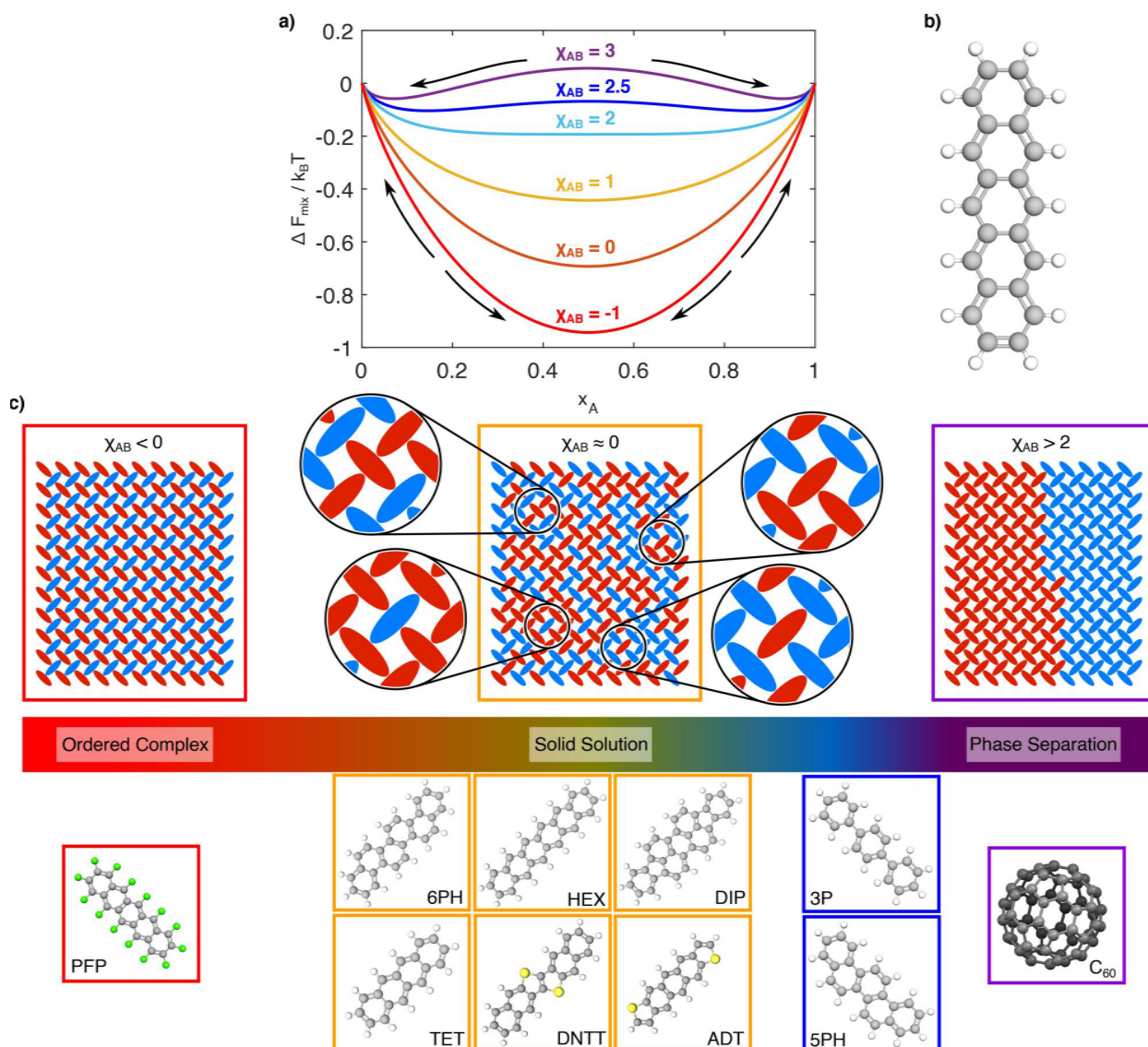


**FIG. 1.** Classification of binary mixtures. (a) Free energy of mixing as derived from a general mean-field approach. (b) Molecular structure of PEN. (c) Top: Illustration of the three types of mixing scenarios (ordered complex, solid solution, and phase separation). For the solid solution, zoom-ins are provided into the nanoscopic arrangement (configuration geometry) of molecules of different types. Note that different length scales can result from the different configurations. Bottom: Molecular structures and assignment to the mixing scenarios of the second molecular compounds that were mixed with PEN. The color coding is red (ordered complex), yellow (solid solution), purple (phase separation), and blue (complex mixing behavior with partial intermixing).

characteristic changes in structural and optical properties are observed for varying mixing ratios. The knowledge gained from these model systems is finally applied to two more challenging binary systems, namely, PEN mixed with [5]phenacene [picene, 5PH, Fig. 1(c)] and with para-terphenyl [3P, Fig. 1(c)]. Their binary blends give rise to mixing scenarios intermediate between the cases presented in the first part. Thus, the entire range between the macroscopic extreme cases of mixing and demixing is covered in this paper by taking into account the mesoscopic order. In the last chapter, the general results

are summarized, and comments are made on the use of multicomponent organic semiconductors in modern optoelectronic devices.

## II. THERMODYNAMIC CONSIDERATIONS FOR BINARY MIXTURES

### A. The regular solution model

A general understanding of the possible mixing scenarios in binary molecular systems (solid solution, phase separation, and ordered complex/co-crystal) can be obtained from thermodynamics,

following the regular solution model in a mean-field approach.<sup>71,72</sup> The derivation is based on a lattice model in which mixing of molecules at the molecular level is only possible via substitutional defects while interstitial mixing is not considered.<sup>73</sup> We shall comment on important deviations and limitations of this equilibrium approach and on more sophisticated theories below. According to the regular solution model, the gain in free energy from the unmixed to the mixed state is given by

$$\Delta F_{\text{mix}} = k_B T \cdot (x_A \cdot \ln x_A + x_B \cdot \ln x_B + \chi_{AB} \cdot x_A x_B), \quad (1)$$

where  $k_B$  is the Boltzmann constant,  $T$  is the temperature, and  $x_A$  ( $x_B$ ) denotes the mole fraction of molecular species  $A$  ( $B$ ). The first two terms describe the entropic contribution, which always favors mixing of the two molecular species, while the third term contains the dimensionless enthalpic interaction balance given by

$$\chi_{AB} = \frac{Z}{k_B T} (W_{AA} + W_{BB} - 2W_{AB}), \quad (2)$$

with  $Z$  being the coordination number defined by the type of lattice. The interaction energies between molecules of the same type are given as  $W_{AA}$  and  $W_{BB}$ , while the interaction between molecules of different types is denoted  $W_{AB}$ . In Fig. 1(a), the dependence of the free energy on the mixing ratio ( $x_A = 1 - x_B$ ) is shown for different values of  $\chi_{AB}$ , which will be discussed next. The full derivation of the mixing free energy [Eq. (1)] using the mean-field approach of the regular solution can be found, for example, in Ref. 72.

## B. Mixing scenarios

Depending on the value of  $\chi_{AB}$  in the expression of the free energy of mixing [Eq. (1)], a categorization of binary systems into the formation of a solid solution, phase separation, and the formation of an ordered complex or co-crystal is obtained [see Fig. 1(c)].<sup>71,74</sup> Note that following its IUPAC definition, and to distinguish it from phase separation and co-crystal formation, we consider solid solutions as a statistical occupation of lattice sites by the two molecular compounds for all mixing ratios. Thus, amorphously mixed systems are not included. If  $\chi_{AB} \approx 0$ , the enthalpic term vanishes, and the gain in free energy upon mixing is determined solely by the mixing entropy. The situation is identical to an ideal solution with the constraint that the lattice sites are statistically occupied by the molecules. It has been emphasized that similarity in size and shape of the two molecular species are necessary conditions for the formation of a solid solution.<sup>71,73,75,76</sup> Importantly, according to the statistical occupation of the lattice sites, all kinds of local nanomolecular environments are encountered for both molecules in a given binary system. This includes isolation of a given molecule from neighboring molecules of the same compound but also more mixed situations. Some illustrative occupancy configurations are shown by the zoom-ins in Fig. 1(c). For an ideal solid solution, their relative abundance is determined solely by the mixing ratio.<sup>24</sup>

The situation changes when  $\chi_{AB}$  becomes increasingly positive, i.e., when the interaction between like molecules dominates the attraction. If  $\chi_{AB} > 2$ , a local maximum is formed at the equimolar mixing ratio [see the purple and dark blue curves in Fig. 1(a)]. To minimize the total free energy, the system separates into two phases in which one molecular species dominates over the other, as indicated by the

arrows. In the limiting case, a separation into neat phases occurs. In contrast to a solid solution, for which the local concentration (except for statistical fluctuations) is identical to the global concentration, for  $\chi_{AB} > 2$ , two phases with constant local concentrations different from the global concentration are obtained whose relative abundance is determined by the global concentration, known as the lever rule.

Finally, if  $\chi_{AB} < 0$ , the interaction energy between dissimilar molecules becomes strongly attractive and outcompetes the interaction between like molecules. Thus, an ordered complex is formed in which the interfacial area between dissimilar molecules is maximized [red curve in Fig. 1(a)]. This ordered complex is still realized when the global concentration deviates from the equimolar mixing ratio, with the molecular species in surplus forming an additional, predominantly pure phase. Note that it is also possible that the combination of two molecular compounds in a stoichiometric ratio different from 1:1 leads to the formation of a stable co-crystal (see, e.g., Refs. 77 and 78). However, such a situation is not captured by the regular solution model.

## C. Beyond regular solution theory

The above derivation of mixing scenarios for changing  $\chi_{AB}$  is based solely on general, fundamental thermodynamic ideas. Nevertheless, it gives a good estimate of the mixing scenarios to be expected in experiments. *A priori* knowledge of the mixing scenario for a given binary system would be of great advantage, for example, by evaluating the interaction parameter  $\chi_{AB}$ , which depends critically on intermolecular interactions. Unfortunately, the prediction of these intermolecular interactions in organic systems goes beyond simple pairwise atomic monopole interactions, as can already be seen from efforts to derive the experimentally accessible polymorphs of a single organic molecular compound.<sup>75,79–81</sup> Note that polymorphism is quite common for van der Waals bound organic crystals due to the weak intermolecular interactions that render the potential energy surface rather shallow.<sup>30,80,82–87</sup> In addition, at least multipole interactions, complex formation by partial charge transfer via orbital hybridization, and Coulombic interactions must be considered.<sup>88,89</sup> Thus, *a priori* knowledge of the mixing behavior is not feasible, and computational approaches that unambiguously predict it are yet to come. Nevertheless, empirical guidelines for estimating the mixing behavior have been established. As mentioned above, similarity in size and shape is a necessary requirement to facilitate the formation of a solid solution.<sup>71,73,75,76</sup> However, also additional effects, such as similarity in the crystal structures of the pristine compounds and similarity in the growth mode during thin-film growth, have been mentioned as possibly influencing the mixing behavior.<sup>73,90</sup> Furthermore, the anisotropy inherent to most organic molecules also induces anisotropic intermolecular interactions, as exemplified by anisotropic exciton transport properties.<sup>91</sup> In turn, these directional intermolecular interactions possibly lead to anisotropic mixing behavior.<sup>66</sup> Thus, the molecular environment in the direct vicinity of a given molecule within a binary mixture can assume distinctly different forms as already illustrated in Fig. 1(c). These various occupational geometries on the nanoscopic length scale result in distinguishable optical and photophysical properties despite the similarity of the macroscopic free energy, as demonstrated in recent TD-DFT calculations and discussed below.<sup>24,92,93</sup>

Additional complexity to the mixing behavior comes from the fact that preparation of mixed thin films, e.g., by OMBD, is a non-equilibrium process.<sup>94–96</sup> For example, the intermolecular interactions may be different in the early stages of crystallization when only a limited number of molecules are in contact.<sup>97</sup> Therefore, adjusting the growth rate can potentially manipulate the mixing behavior by inducing a change in the growth kinetics, with a higher deposition rate generally facilitating better mixing. Furthermore, adjusting the substrate temperature not only affects  $\chi_{AB}$ , but also changes the diffusion dynamics of adsorbed molecules, thus altering the kinetics. The relevance of kinetic aspects might be further strengthened by using non-classical strategies in thin-film preparation by OMBD, such as interrupted growth or growth under glancing angle.<sup>98–100</sup> Additionally, growth under illumination with polarized light might open further possibilities to manipulate growth and mixing in single-component and binary mixed thin films.<sup>101</sup>

To summarize this section, there are three different general mixing scenarios for binary molecular mixtures, namely, the formation of a solid solution, phase separation, and the formation of an ordered complex. Although similarity in size and shape of the molecules appears to be a necessary requirement for the formation of a solid solution, the situation is more intricate. In addition to the anisotropy in intermolecular interactions that is inevitable for anisotropic molecules, it should further be kept in mind that the preparation of binary mixtures by thin-film growth adds kinetic aspects to the thermodynamic considerations.

### III. PRISTINE PEN

Before discussing the structural and optical properties of PEN in binary organic mixtures, we briefly summarize the respective properties of pristine PEN.

#### A. Structural properties

In accordance with its molecular structure [Fig. 1(b)], PEN is classified as a rigid, rod-like organic molecule. Several polymorphs of the PEN crystal structure are known to exist.<sup>86,102–109</sup> Most relevant to this paper is the thin-film polymorph obtained for growth on

weakly interacting substrates such as silica and glass, due to the preparation technique and conditions used.<sup>104</sup> During sample preparation by OMBD at room temperature, PEN molecules adopt an almost perfect upright-standing orientation on weakly interacting substrates [see inset in Fig. 2(a)]. This can be deduced, for example, from the position of the Bragg reflections in the XRR diffraction data [Fig. 2(a)]. Slight differences in tilt angles for PEN molecules within the first monolayer and subsequent layers, as well as for variations in substrate temperature during deposition, have been reported.<sup>110–113</sup> For larger film thicknesses, a transition to the bulk phase polymorph of PEN occurs.<sup>107,114–116</sup> We note that the situation is not very different from several other rod-like organic semiconductors, such as TET and DIP, so that these considerations can be transferred with some level of generality.<sup>7,74,83,117–120</sup>

The primitive unit cell is triclinic and contains two translationally inequivalent molecules. Additional crystal lattice parameters can be derived from grazing incidence x-ray diffraction (GIXD) data, as shown in Fig. 2(b). The vertical lines shown there correspond to the lattice parameters reported for the thin-film crystal structure of PEN.<sup>104</sup> Therein, it is assumed that the *ab*-plane is oriented parallel to the substrate. From the peak intensities, information about the atomic positions within the unit cell can be obtained. For PEN, all-atom resolved literature data exist for both the thin-film and bulk crystal structures.<sup>102,104,106,121</sup> PEN molecules adopt a herringbone packing motif as illustrated in the inset of Fig. 2(b).

#### B. Optical properties

The structural properties and especially the orientation of the molecules with respect to each other as described by the crystal structure have a strong impact on the optical properties. In essence for PEN, the two translationally inequivalent molecules per unit cell give rise to a splitting in the lowest optical electronic transition at 1.87 and 1.97 eV [Fig. 2(c)], referred to as Davydov splitting.<sup>122</sup> This splitting is due to a coupling of the molecular transition dipole moments and leads to J- and H-aggregate-like behavior in the two Davydov components.<sup>26,123,124</sup> Importantly, in addition to the dipole-moment coupling known as Coulomb coupling, contributions from charge-

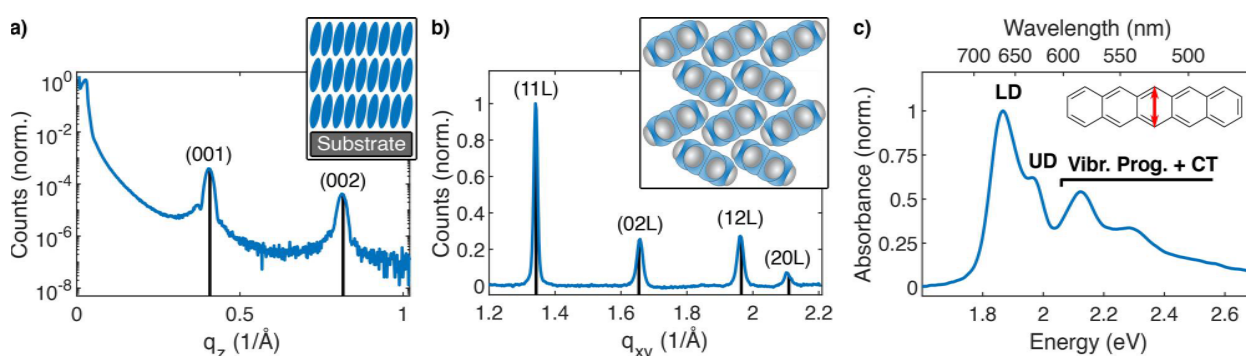


**FIG. 2.** Structural and optical properties of pristine PEN. (a) and (b) X-ray diffraction data obtained in XRR and GIXD geometry with diffraction peaks labeled by their Miller indices. Vertical lines correspond to the reported thin-film crystal structure of PEN.<sup>104</sup> Insets illustrate the nearly upright-standing orientation of PEN molecules on weakly interacting substrates and the in-plane herringbone packing motif. (c) UV/vis absorption spectrum of pristine PEN. Absorption bands corresponding to the lower (LD) and upper (UD) Davydov components are labeled. Optical features above UD have been assigned to electronic transitions to charge-resonance states and to a vibronic progression of the  $S_1 \leftarrow S_0$  optical transition. The orientation of the transition dipole moment along the short axis of the molecular plane corresponding to this electronic transition is indicated in the molecular structure of PEN.

resonance interactions also contribute to Davydov splitting in solid PEN.<sup>26,92,125–130</sup> Note that while in the literature these states are frequently referred to as charge-transfer states, we reserve this term for strongly non-symmetric interactions as observed in donor–acceptor pairs. Instead, the term “charge-resonance” used here, which has been used, for example, in Refs. 131 and 132, highlights the coupled nature of these states. These charge-resonance electronic transitions have been reported slightly above the optical bandgap, starting at 2.12 eV.<sup>133</sup> However, field-modulation spectroscopy experiments have indicated that these reported experimental values could also be the result of charge accumulation during the measurement, and instead charge-resonance states may only exist above 2.7 eV.<sup>134</sup> It is, therefore, not surprising that the peak at 2.12 eV has instead also been assigned to a vibronic progression.<sup>135</sup> It seems likely that both transitions to charge-resonance states and electronic states containing vibrational quanta contribute to that optical signal.<sup>92,93</sup>

The above considerations apply to PEN in crystal structures. They, therefore, are essential to understand the optical properties in the ordered solid state. In addition, for thin-film growth, the substrate frequently induces uniaxial orientational order that has further implications on the measured absorption spectrum, in essence, for the here discussed illumination under normal incidence. This can be appreciated most easily already from the orientation of the transition dipole moment of the single molecule. Note, however, that in the solid state, Coulomb and charge-resonance intermolecular coupling modify both the strength and direction of these transition dipole moments, which will be discussed below. The electronic and vibronic states of the single molecule enter the description of the optical properties in the solid state as diabatic Frenkel states. Thus, a general understanding of these molecular electronic states and especially transitions between them are essential to fully understand the optical absorption spectrum of pristine PEN.

The orientation of the single-molecule transition dipole moment depends on the symmetry of both the initial and final electronic state. For example, the molecular transition dipole moment for the  $S_1 \leftarrow S_0$  electronic transition in isolated PEN is oriented along the short axis of the molecular plane [see inset in Fig. 2(c)].<sup>127,136,137</sup> Thus, for vertical illumination of unpolarized light, the interaction between the electromagnetic wave and the upright-standing molecules is maximized, resulting in strong absorption for this optical transition. Importantly, this directionality with respect to the substrate is still preserved if Coulomb coupling to neighboring PEN molecules is considered, as the vector addition of the molecular transition dipole moments of the two translationally inequivalent molecules per unit cell remains being oriented perpendicular to the surface normal.<sup>59,135</sup> However, if the orientation of the molecules on the substrate is changed, the anisotropic nature of the single-molecule properties also changes the bulk optical and electronic properties.<sup>138–141</sup>

In contrast to the  $S_1 \leftarrow S_0$  transition, the transition dipole moment of the next higher optically allowed transition in PEN (denoted  $S_3 \leftarrow S_0$  in Ref. 93) is oriented along the long molecular axis.<sup>93,136,142</sup> According to quantum chemical calculations, it has a much higher oscillator strength compared to the transition from  $S_0$  to  $S_1$ .<sup>93,136,142</sup> However, these calculations predict this transition of being located at energies most likely above 4 eV. Thus, transitions to  $S_3$  are not of relevance for this paper in which we focus on the impact of the mixing behavior on the low-energy optical transitions that are also

**TABLE I.** Molecular dimensions according to the reported crystal structures assuming van der Waals radii for the edge atoms. The relative dimension, with PEN serving as the reference, is given in percent.

| Compound            | Long axis |     | Short axis |     |
|---------------------|-----------|-----|------------|-----|
|                     | (Å)       | (%) | (Å)        | (%) |
| PEN <sup>102</sup>  | 14.1      | 100 | 4.9        | 100 |
| TET <sup>102</sup>  | 11.6      | 82  | 4.9        | 100 |
| HEX <sup>151</sup>  | 16.5      | 117 | 4.9        | 100 |
| ADT <sup>152</sup>  | 14.0      | 99  | 5.0        | 102 |
| DNTT <sup>153</sup> | 15.6      | 111 | 5.7        | 116 |
| 6PH <sup>a</sup>    | 16.0      | 113 | 5.6        | 114 |
| 5PH <sup>154</sup>  | 13.7      | 97  | 5.8        | 118 |
| 3P <sup>150</sup>   | 13.5      | 96  | 4.2        | 86  |

<sup>a</sup>Approximate value based on a comparison with its smaller homologs 4PH (crysens) and 5PH.<sup>154,155</sup>

most relevant for optoelectronic applications. Likewise, the optical transition from  $S_0$  to the optically dark  $S_2$  state, which is symmetry forbidden, is not further discussed, and the interested reader is referred to the literature where the  $S_2$  state has received considerable attention due to its potential role as an intermediate state in the singlet exciton fission process in PEN.<sup>143–146</sup>

### C. Growth mode and molecular dimensions

During thin-film sample preparation by OMBD, PEN follows the Stranski–Krastanov growth mode for deposition around room temperature.<sup>147–149</sup> Within the first few monolayers, the substrate is completely covered by PEN molecules before island formation sets in at subsequent layers. As mentioned in the introduction, differences in growth mode could be responsible for the induction of phase separation in binary mixtures.<sup>96</sup> The different mixing scenarios obtained for different organic binary systems are the subject of the following sections. The molecular dimensions, derived from the atomic distances in the crystal structures of the molecules used, are listed in Table I. With the exception of Buckminster fullerene ( $C_{60}$ ), the molecules used have a rod-like shape. The dimensions within the molecular plane defined by the  $\pi$ -system are listed. Note that even 3P, the only non-rigid molecule discussed in this paper, adopts a rather planar structure in the crystalline state, thus allowing for direct comparison with the molecular structure of PEN.<sup>150</sup> For [6]phenacene (fulminene, 6PH), no atomically resolved crystal structure has been reported in the literature. However, approximate molecular dimensions for 6PH can be deduced by comparison with the reported crystal structures of its smaller homologs.

### IV. SOLID SOLUTION

The formation of a solid solution containing PEN as one of the two compounds has been reported for several binary systems. These include TET, hexacene (HEX), DIP, anthradithiophene (ADT), 6PH, and dinaphthothienothiophene (DNTT) as the second molecular species.<sup>13,15,24,58,59,65,66,156</sup> Their molecular structures are shown in Fig. 1(c). In all of these systems, the requirement of similarity in size and shape of the rod-like molecules, a prerequisite for the statistical

occupation of lattice sites by substitutional disorder,<sup>73</sup> is reasonably well satisfied (see Table I). Furthermore, neither integer nor partial charge transfer between PEN and the second molecular species seems likely based on the respective energy of the frontier molecular orbitals and the electron affinity and ionization potential.<sup>13,119,157–159</sup> Therefore, it can be expected that weak intermolecular interactions of the van der Waals type dominate, both between like ( $W_{AA}$  and  $W_{BB}$ ) and dissimilar ( $W_{AB}$ ) molecules. The second molecular compounds used are, likePEN, hydrocarbon molecules. DNNT and ADT additionally contain two sulfur atoms, respectively, in their molecular structure. Importantly, none of the molecules contain any electron-donating (e.g., amino or hydroxyl groups) or electron-withdrawing groups (e.g., fluorine atoms or cyano groups). Thus, a similar charge distribution between the periphery and the bulk of the molecules can be expected, resulting in comparable intermolecular interactions between like and dissimilar molecules in the mixed crystal state. Taken together, these rather crude energetic considerations support the expectation of the formation of solid solutions in these binary systems.

### A. Structural properties

The typical structural features for solid solutions containing PEN are demonstrated based on XRR data for PEN:TET blends of 20 nm thickness (Fig. 3).<sup>24</sup> First, pronounced Bragg peaks are observed for all blend ratios. This clearly demonstrates that a crystalline structure is maintained in the blends and that there is no transformation to an amorphous structure. The similarity in the width of the Bragg peaks further demonstrates that this crystalline order extends throughout the film thickness.<sup>160</sup>

Most important for the deduction of the formation of a solid solution from the data presented in Fig. 3 is the position of the Bragg peaks, which gives information about the out-of-plane lattice spacing. This spacing is quantified in Fig. 3(b). In solid solutions, a continuous change in the lattice parameters is observed for the changing mixing ratio.<sup>161</sup> However, our data for PEN:TET blends also indicate that deviations from the linear trend, as predicted by Vegard's empirical law,<sup>162</sup> are possible. This is likely to be the result of the weak intermolecular interactions typically present in organic crystals and the inherent complexity due to the increased degrees of freedom for extended molecules compared to single atoms. In particular, non-rigid molecules can, to some extent, adapt their molecular structure in the solid state to increase packing density and attractive intermolecular interactions.<sup>163–165</sup> Furthermore, the anharmonic potential in intermolecular interactions renders it energetically more favorable to dissolve a smaller molecule in the lattice of larger molecules than vice versa, resulting in a deviation to larger lattice spacings compared to the linear trend.<sup>75,166</sup> Note that also the possibility for a deviation to smaller lattice parameters has been reported in the literature for other organic binary mixtures.<sup>166</sup> However, we speculate that this is only possible for systems containing less rigid molecules or if the molecular geometry deviates from rod-like molecules, allowing for the formation of cavities that can be filled by the second molecular compound.

The mixing of multiple molecular compounds most frequently increases disorder in the system. This is especially important for electronic and optoelectronic devices, as disorder has an impact on the conductivity.<sup>167,168</sup> As such, both the short-range occupational geometry and the mesoscopic crystalline ordering and crystal grain

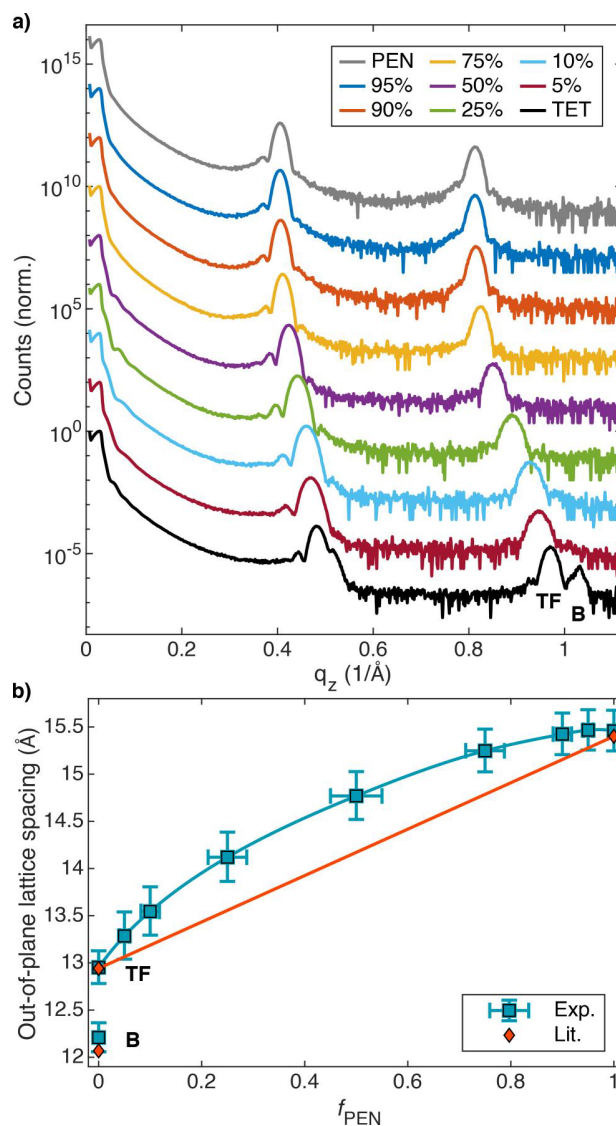


**FIG. 3.** Structural properties in solid solutions containing PEN and TET. (a) Normalized XRR diffractograms displayed with offset for clarity. The presence of diffraction peaks indicates the presence of a crystalline structure. (b) Corresponding out-of-plane lattice spacing. The continuous trend of the lattice spacing with  $f_{PEN}$  is characteristic for the formation of a solid solution. For pristine TET, both the thin-film (TF) and bulk (B) crystal structures are present. See text for details, including the observed deviation from the linear change in lattice spacing predicted by Vegard's law. Reprinted with permission from Unger *et al.*, *J. Phys. Chem. A* **128**(4), 747–760 (2024). Copyright 2024 American Chemical Society.<sup>24</sup>

boundaries are critical parameters. While the former should follow statistical arguments in solid solutions, the latter can be investigated by probing the coherent scattering size that further serves as a measure of the defect density.<sup>25</sup> An imposing example for this is shown in Fig. 4 for blends of PEN with DIP.<sup>66</sup> The coherent scattering size has been determined from the analysis of the Bragg peak widths in GIWAXS data using the Scherrer equation.<sup>160</sup> Note that this probes

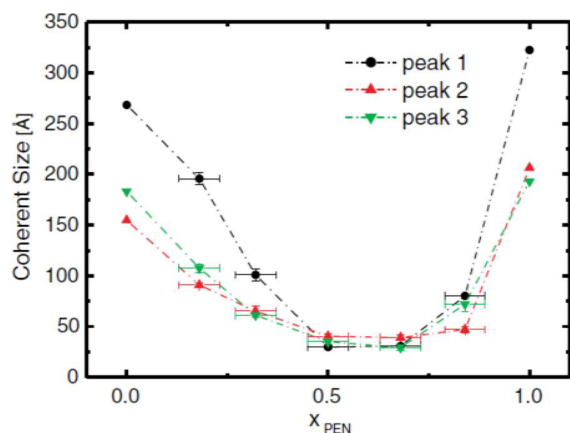


**FIG. 4.** In-plane coherent scattering size for PEN:DIP blends. Reprinted with permission from Aufderheide *et al.*, *Phys. Rev. Lett.* **109**, 156102 (2012). Copyright 2012 American Physical Society.<sup>66</sup>

the disorder in the in-plane direction. For thin-film blends of small thickness, the out-of-plane coherent scattering size is frequently limited by the film thickness, as can be concluded from the identical widths of Bragg peaks in XRR experiments as, for example, seen in Fig. 3. Also for PEN:DIP blends, the coherent scattering size along the out-of-plane direction remains robust, independent of the mixing ratio.<sup>66</sup> In contrast, a strong reduction in the in-plane coherent scattering size at intermediate mixing ratios has been observed.<sup>66</sup> Thus, it has been concluded that the system behaves analogously to a liquid crystal adopting a smectic phase. Furthermore, it illustrates that the inherent anisotropy in non-spherical molecules induces anisotropic ordering in the mixed thin films. We note that while a reduction in ordering is frequently encountered in binary mixed systems, it is also possible that the mixing increases the ordering and thus can be exploited to improve conductivity and ultimately device performance (see Ref. 1 and references therein).

## B. Optical properties

A central focus of this paper is to relate the mixing behavior derived from a structural analysis to the optical properties. For solid solutions this is demonstrated using PEN:6PH blends (Fig. 5).<sup>13</sup> The PEN absorption bands below 2.7 eV have been labeled ( $P_1$ – $P_4$ ) for an easier discussion of the observed trends. They can be related to the absorption bands in neat PEN as discussed above, but changes occur in the blends. First, a change in the relative intensities of the first two peaks [ $P_1$  and  $P_2$ , being analogous to the lower and upper Davydov components in neat PEN, respectively, see Fig. 2(c)] is observed. As demonstrated in Ref. 24, this is mainly due to a broadening of the absorption band  $P_1$ . The occupational disorder in the solid solution perturbs the lowest optical transition in PEN due to the nature of the electronic state describing the lower Davydov component, which is delocalized over many molecules and contains large contributions from charge-resonance interactions.<sup>24,169</sup> Thus, this state is strongly susceptible to the static disorder introduced by the presence of the second molecular compound.<sup>57</sup> In contrast, in the binary blends,  $P_2$  contains spectral contributions from predominantly Frenkel H-type-like electronically coupled PEN

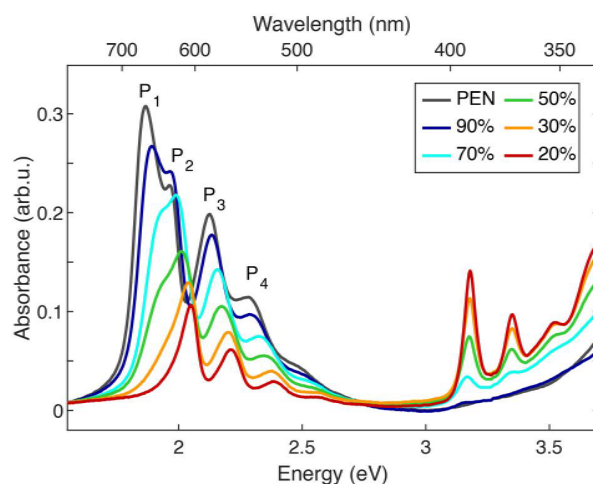


**FIG. 5.** Optical properties in PEN:6PH solid solutions. Lowest absorption bands related to excitons predominantly localized on PEN molecules are labeled  $P_1$ – $P_4$ . Adapted with permission from Unger *et al.*, *J. Am. Chem. Soc.* **144**(45), 20610–20619 (2022). Copyright 2022 American Chemical Society.<sup>13</sup>

molecules, consistent with the upper Davydov component, plus signatures from electronically mostly decoupled PEN molecules. Importantly, the charge-resonance character of  $P_1$ , the absorption band corresponding to the lower Davydov component in neat PEN, is expected to be greatly reduced, as deduced from the comparison of experimental and computational data.<sup>24,58</sup> Since the charge-resonance character is responsible for the Davydov splitting (the energetic difference between  $P_1$  and  $P_2$ ),<sup>128</sup>  $P_1$  shifts closer in energy to  $P_2$ .

In the region of the higher energy absorption bands  $P_3$  and  $P_4$ , a multitude of electronic transitions has been predicted to exist by quantum chemical calculations on PEN:TET blends.<sup>24</sup> The corresponding excitonic states have been shown to differ greatly in their diabatic charge-resonance character. However, these calculations have also indicated that electronic transitions by themselves are insufficient to describe the experimentally observed absorption bands. Therefore, additional contributions from vibronic satellites can be expected to play a non-negligible role in this energy region. This is further supported by their congruent hypsochromic shift observed in the blends in Fig. 5 for decreasing PEN concentration. Taken together, a complex mixture of electronic and vibronic states that can be composed of both Frenkel and charge-resonance character is required to explain the absorption bands  $P_3$  and  $P_4$ . This is in agreement with experimental electron energy loss and computational results for neat PEN,<sup>127,170</sup> thus demonstrating the ability of using binary mixtures for a better understanding of the properties of the neat compounds.

Interestingly, all of the solid solutions discussed in this paper show similar trends in the absorption features originating from PEN molecules. These include (i) the changes in the relative peak intensities of the absorption bands  $P_1$  and  $P_2$ , (ii) the reduction of Davydov splitting, and (iii) the hypsochromic shift to higher energies.<sup>13,24,58</sup> Thus, due to the latter, a tuning of optical properties in PEN becomes accessible through the use of solid solutions. The similar trends in the binary mixtures indicate that the observed changes are the result of a statistical substitutional disorder, and most of the changes that occur

can be understood qualitatively independent of the nature of the second molecular compound. Instead, the nanoscale short-range order in the sense of occupational configuration geometries possibly explains the optical response in binary blends containing PEN in great parts. This has been demonstrated in Ref. 24 by TD-DFT calculations on molecular clusters containing eight molecular sites occupied by PEN and TET molecules. Depending on the occupational geometry by the two molecular species, optical transitions to electronic states at different energies can occur. Importantly, it became possible to greatly reproduce the experimentally observed absorption spectrum for an intermediate mixing ratio by a linear combination of these absorption spectra. Thus, the optical properties in solid solutions are affected by the occupational geometry of lattice sites by the two molecular species. While the trend in absorption band intensities and reduction in Davydov splitting seems general for PEN-based solid solutions, there are also subtle differences between the statistically mixing binary systems. Especially the magnitude of the hypsochromic shift strongly depends on the choice of the second molecular compound.<sup>13</sup> As demonstrated in Ref. 13, the main cause of the strength of this shift is a change in polarizability in the direct vicinity of PEN molecules by occupation of lattice sites by molecules of the second molecular compound. Empirically, a relation between optical bandgap and polarizability has been found, which has been confirmed by theoretical calculations on 2D materials.<sup>171,172</sup> It seems likely that PEN is exceptionally suitable for tuning its optical properties by a change in the polarizability of the molecular environment due to the pronounced delocalization and separation of the electron-hole pair in the lowest electronically excited states, exemplified by large contributions from charge-resonance states.<sup>4,92,93,127–130,169</sup>

### C. Conclusion

Taken together, the solid solutions discussed in this paper can be characterized by the following criteria: (i) The molecules are mixed by statistical occupation of lattice sites, with the proportions of constituents being able to be varied over the entire range of mixing ratios. Based on the energy level alignment of frontier molecular orbitals and charge distribution in the molecules, no chemical reaction between the molecular compounds is expected. A nice proof of the chemical stability has been demonstrated for a comparable binary organic mixture containing PEN by dissolution of the deposited thin film in a suitable solvent.<sup>173</sup> In the solution, the intact molecules were recovered, while no indication for any new molecular species was obtained. (ii) Continuous changes in structural and optical properties with respect to the mixing ratio occur that cannot be described as a superposition of the properties inherent to the constituents. This includes the position and relative intensities in the Davydov components. (iii) As has been demonstrated theoretically in Ref. 24, wave functions describing the lowest electronic states accessible in optical absorption experiments of PEN:TET solid solutions are located on PEN and TET molecules simultaneously, both with Frenkel and charge-resonance character. Thus, electronic coupling between molecules of different compounds seems likely. Importantly, these criteria recently have been postulated as a necessary requirement for the classification of a binary mixture as an “organic alloy.”<sup>174</sup> While we do not intend to engage in a debate on semantics, our results suggest that binary solid solutions containing PEN are the first examples of organic alloys so far meeting these criteria. In contrast to the mixtures containing

spherical fullerene molecules discussed in Ref. 174, the rod-like, compact shape of PEN molecules facilitates stronger electronic coupling to neighboring molecules, manifesting in charge-resonance contributions in the lowest electronically excited states of pristine PEN.<sup>92,93,127–130,169</sup> In the binary blends, this electronic coupling is distorted by the second compound molecules. While electronic coupling between PEN and TET molecules has been calculated to exist in the respective solid solutions, even the case of vanishing electronic coupling to molecules of dissimilar types can be considered a limiting case of intermolecular electronic coupling.

## V. PHASE-SEPARATING SYSTEMS

As structural similarity is a precondition for the formation of solid solutions,<sup>73</sup> it is a natural choice to use a molecule structurally dissimilar to PEN to investigate PEN in phase-separating systems. Therefore, it is no surprise that blending rod-like, flat PEN with spherical, bulky C<sub>60</sub> Buckminsterfullerene [molecular structure shown in Fig. 1(c)] results in phase separation.<sup>25,67,68,175</sup> The combination of these materials has attracted considerable interest as a donor-acceptor system for application in organic solar cells.<sup>176–178</sup>

### A. Structural properties

In Fig. 6, out-of-plane x-ray diffraction curves are shown for 30 nm thick PEN:C<sub>60</sub> blends of varying mixing ratio.<sup>68</sup> Their observation of a Bragg peak doublet for the neat PEN sample with the diffraction peaks corresponding to the thin film and bulk phase indexed by (00L') and (00L), respectively, is somehow surprising. While signatures from the bulk phase are typically observed only at slightly larger film thicknesses, this might be due to some differences in preparation conditions, here in particular, a pretreatment of the silicon substrates to remove the native oxide layer.<sup>115,116</sup> Interestingly, only the thin-film phase of PEN is present in the blends with C<sub>60</sub>.

Typical for a phase-separating system is the robustness of the Bragg peak positions in the diffractograms, independent of the mixing

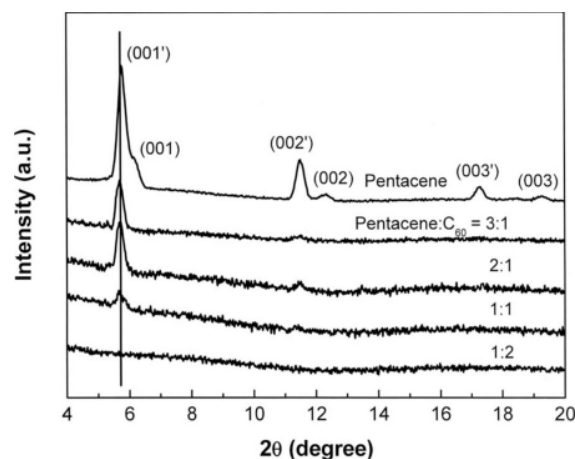


**FIG. 6.** Structural properties in phase-separating PEN:C<sub>60</sub> blends. The position of the Bragg peaks remains unchanged. A larger structural disorder, induced by increasing C<sub>60</sub> concentration, results in the disappearance of Bragg reflections. See text for details. Reprinted with permission from Zheng *et al.*, *J. Vac. Sci. Technol. B* 27(1), 169–179 (2009). Copyright 2009 American Vacuum Society.<sup>68</sup>

ratio. Especially for a binary system containing such structurally dissimilar molecules as PEN and  $C_{60}$ , a separation into the (almost) pure phases seems likely. Within these phases, the pristine crystal structures are obtained.

Under the conditions used in Ref. 68,  $C_{60}$  was said to grow amorphous, not giving rise to any Bragg peak in its diffractogram. We note, however, that this could also be the result of a non-uniaxial orientation of  $C_{60}$  crystallites, distributing the x-ray scattering intensity over the entire range of azimuth angles and thus strongly decreasing the Bragg reflection intensity in an XRR experiment. In the PEN: $C_{60}$  blends, the intensity of the PEN diffraction peaks becomes smaller for increasing  $C_{60}$  concentration, which is the result of an increased structural disorder. This can be both the induction of an amorphous PEN phase or a change in crystal orientation away from the uniaxial directionality induced by the substrate due to amorphous or isotropic polycrystalline  $C_{60}$ . PEN, on the contrary, can also act as a templating layer for on-top deposition of  $C_{60}$  in which case a known polymorph of  $C_{60}$  is obtained, therefore increasing the crystalline order in  $C_{60}$ .<sup>175</sup> An additional explanation for the reduced structural order in the samples reported in Ref. 68 could be a possible Diels–Alder reaction between the two molecular compounds as demonstrated in Ref. 179. The chemical reaction, which predominantly occurs at the interfacial region, gives rise to a new molecular species with a distinct molecular structure. This induces an additional disorder in the blended structure, lowering the intensity of Bragg peaks.

## B. Optical properties

Similar to the robustness of the Bragg peaks in the x-ray diffractograms, the absorption bands in phase-separating PEN: $C_{60}$  blends also remain at similar energies (see Fig. 7).<sup>67</sup> The two Davydov components of PEN can be clearly resolved, also in the blend, with a higher intensity of the energetically lower Davydov component at 670 nm (1.85 eV). In combination with identical Davydov splitting in the pristine PEN film and the PEN: $C_{60}$  blend, this is in stark contrast to the situation in solid solutions as discussed above, for which Davydov splitting becomes smaller for a decreasing amount of PEN and the energetically lower Davydov component loses in intensity. Focusing on the absorption features attributable to PEN, the minor peak shifts observed in Fig. 7 are likely to be explained by the instrumental resolution, and differences in the absorption spectra for the PEN thin-film and bulk phase polymorphs (compare with Refs. 180 and 181). As shown above in the discussion of the structural properties, the abundance of these two polymorphs is altered in the pristine and blended film. Other possible explanations include polarization effects from the phase-separated  $C_{60}$  phase and differences in strain for the two samples.

The lower intensity of PEN absorption bands in the blend compared to the pristine film is likely to be caused by the reduced orientational order caused by the presence of the amorphous  $C_{60}$  phases. In neat PEN samples, the close to upright-standing orientation of PEN molecules with respect to the substrate maximizes the absorption intensity at the optical bandgap for illumination under normal incidence. An increased orientational disorder of PEN molecules away from the substrate-normal, induced by the amorphous  $C_{60}$  phase, inevitably also lowers the absorption intensity. Nevertheless, clear and pronounced Davydov splitting is indicative of a crystalline short-range ordering in the PEN phase.<sup>142</sup> The formation of an amorphous

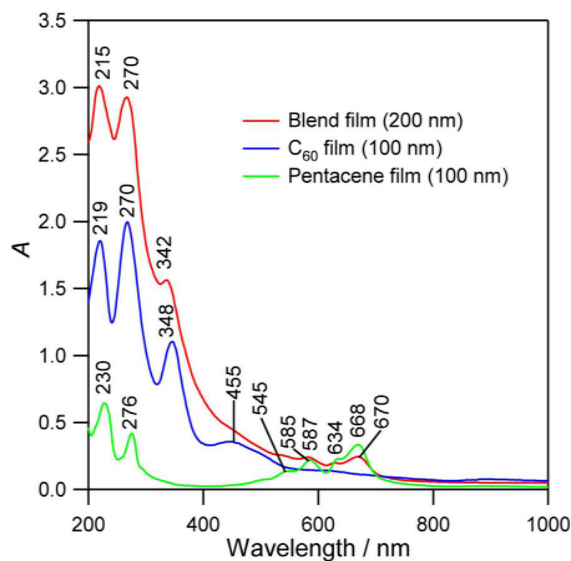


**FIG. 7.** Optical properties in phase-separating PEN: $C_{60}$  blends. In contrast to the optical absorption spectra for solid solutions, shifts in absorption bands attributable to PEN are minimal and can be attributed to the instrumental resolution and the different abundance of the PEN thin film and bulk polymorph in the pristine and blended film (compare with Refs. 180 and 181). Additionally, polarization effects from phase-separated  $C_{60}$  and differences in stress in the organic layer possibly contribute to these differences. The lower absorbance in the blended film might be attributable to the lower orientational order of PEN crystallites induced by the amorphous structure of  $C_{60}$ . See text for details. Reprinted with permission from Iwasawa and Furukawa, Chem. Phys. Lett. 636, 58–61 (2015). Copyright 2015 Elsevier.<sup>67</sup>

PEN phase would cause the breakdown of the Davydov splitting, much as has been observed for TIPS-PEN nanoparticles for which the structural ordering has been increased via thermal and solvent annealing.<sup>182</sup> Therefore, the optical absorption data indicate that despite the absence of strong Bragg reflections in the XRR diffractograms of the equimolar PEN: $C_{60}$  blend, a regularly ordered, separated PEN phase is formed. However, these PEN-rich crystallites might be oriented isotropically within the organic thin film in contrast to the uniaxial orientation of PEN molecules in the pristine thin film. Thus, the information deduced from UV/vis absorption experiments can serve to complement structural information obtained from x-ray diffraction experiments. While UV/vis absorption for organic solids is mainly sensitive to the single-molecule properties in combination with the intermolecular interaction with neighboring molecules in direct vicinity,<sup>57</sup> x-ray diffraction around the Bragg peak typically probes the long-range ordering and scales with the number of scatterers squared.

As already mentioned above, blending PEN with the structurally highly dissimilar  $C_{60}$  molecule is an obvious choice for realizing a phase-separated system. Likewise, co-deposition of rod-like organic molecules that strongly differ in their molecular dimension(s) results in phase separation,<sup>89,183</sup> thus highlighting the importance of structural similarity on the mixing behavior. However, we would like to point out that phase separation is also possible for geometrically rather similar molecules. For example, PEN phase-separates from 6,13-pentacenequinone as concluded from x-ray diffraction and

atomic force microscopy.<sup>90</sup> There, the preference for phase separation, despite high structural similarity of the molecules, has been attributed to differences in the crystal structure and the growth mode of the two molecules, both being the result of a change in intermolecular interaction. Furthermore, the tendency for phase separation in a system can be reduced by increasing the intermolecular interaction between the two molecular species,<sup>89</sup> which ultimately can result in the formation of a co-crystal as discussed next.

## VI. CO-CRYSTAL FORMATION

The formation of a co-crystal in organic binary systems has been investigated thoroughly by combining PEN with its perfluorinated analog, PFP [molecular structure shown in Fig. 1(c)].<sup>61,62,110,184–190</sup> Both are structurally highly similar, facilitating intermixing on the molecular level. In addition, the fluorination of the PEN molecular backbone results in an inversion in its quadrupole moment,<sup>191</sup> causing an attractive interaction between the two molecules. This has been demonstrated experimentally, using thermal desorption spectroscopy.<sup>186</sup> The increase in thermal stability is particularly detected for the equimolar blend, indicating the formation of an ordered co-crystal with alternating PEN and PFP molecules. Therefore, we first discuss the structural and optical properties of the equimolar PEN:PFP blend before turning to mixing ratios deviating from it.

### A. Structural properties of equimolar blends

In Fig. 8, GIXD scans of PEN:PFP blends from Ref. 62 are shown. In the equimolar blend, new Bragg reflections occur that cannot be explained by either of the two compounds.<sup>62,184</sup> Furthermore, in contrast to systems forming solid solutions as discussed above, these new diffraction peaks cannot be assigned to continuous changes in the lattice parameters.<sup>18</sup> This will become clearer still when discussing the non-equimolar mixing ratios below. The crystal structure formed in the equimolar PEN:PFP blend attracts considerable interest as it forms the basis for discussions of the photophysical properties in that blend as well as the process of charge separation at the interface between PEN and PFP in planar-heterojunction devices. Even though a full characterization of all atomic positions within the unit cell has not been reported so far, comparison between experimental GIXD data and computational force-field calculations has indicated that the co-crystal unit cell contains two cofacial molecules.<sup>189</sup> This cofacial orientation is in agreement with the expectations from the inverted quadrupole moment upon fluorination of PEN<sup>191</sup> and also explains the optical absorption properties in the equimolar blend as detailed next.

### B. Optical properties of equimolar blends

Optical absorption spectra of PEN:PFP blends obtained from spectroscopic ellipsometry are shown in Fig. 9, reproduced from Ref. 61. In the equimolar blend (black curve), a new optical feature arises below the optical bandgap of pristine PEN and pristine PFP, just below 1.6 eV.<sup>61,192</sup> Thus, it belongs to a new electronic transition, which has been assigned to the formation of a charge-transfer exciton.<sup>61,185,188,189</sup> This charge-transfer electronic state is expected to be the result of molecular orbital hybridization based on the similarity of the molecules as detailed in Ref. 50. The molecular orbital interaction is believed to be maximal for a cofacial orientation of the two rod-like molecules for which orbital overlap is maximized. Support for that

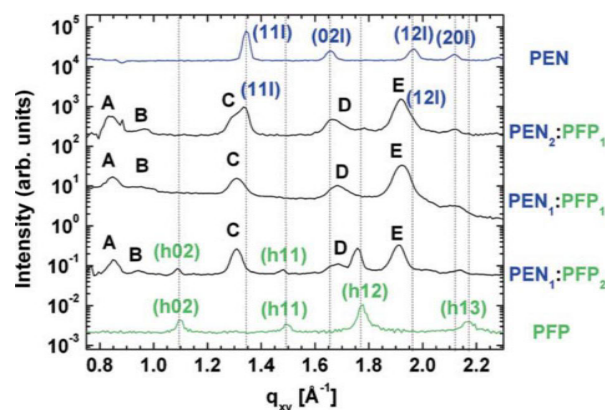


**FIG. 8.** Structural properties in PEN:PFP blends forming co-crystals. Additional diffraction peaks (labeled A–F) occur in the GIXD data of the blends that cannot be explained by the neat compounds' crystal structures. These diffraction peaks are characteristic for the formation of a PEN:PFP co-crystal and, for non-equimolar mixing ratios, coexist together with diffraction peaks characteristic for the neat phases. See text for details. Reprinted from Hinderhofer *et al.*, *J. Chem. Phys.* **134**(10), 104702 (2011) with the permission of AIP Publishing LLC.<sup>62</sup>

has further been obtained experimentally from a comparison of the strength in the low-energy, optical charge-transfer transition for different orientations of the molecules in a layered thin-film architecture.<sup>188,193</sup> This has been achieved by comparing samples obtained from on-top deposition with blended thin films<sup>193</sup> and by switching between standing-up and lying-down orientation of the deposited molecules in planar-heterojunction devices.<sup>188</sup>

While there is conclusive evidence that the low-energy absorption feature at 1.6 eV is the result of charge-transfer complex formation between the HOMO of the donor-PEN and the LUMO of the acceptor-PFP molecule, a clear assignment of the absorption features above that energy is challenging. This is due to the overlapping absorption spectra of PEN and PFP.<sup>192</sup> Attempts to separate the features and attribute them to electronic transitions predominantly located on either PEN or PFP made use of slight differences in molecular tilt angle for different deposition temperatures as confirmed by NEXAFS.<sup>110</sup> However, it should be noted that such an assignment to one of the two molecular compounds might be impossible if the strong electronic intermolecular interaction between the two compounds is not only present in the lowest optical transition but also in optical transitions that involve other molecular orbitals of different symmetry.

### C. Conclusion for equimolar blends

Taken together, the structural and optical properties of the equimolar PEN:PFP blend show clear formation of a co-crystal with one PEN and one PFP molecule per unit cell in a cofacial orientation. Further support is obtained from the evolution in roughness for the changing mixing ratio in the system, which shows a spike of higher roughness for the equimolar mixing ratio.<sup>25</sup> The HOMO of PEN and LUMO of PFP hybridize to form two new intermolecular orbitals composing the charge-transfer state. The formation of a co-crystal suggests a strong intermolecular interaction between PEN and PFP molecules, resulting in thermal stabilization of the equimolar mixing

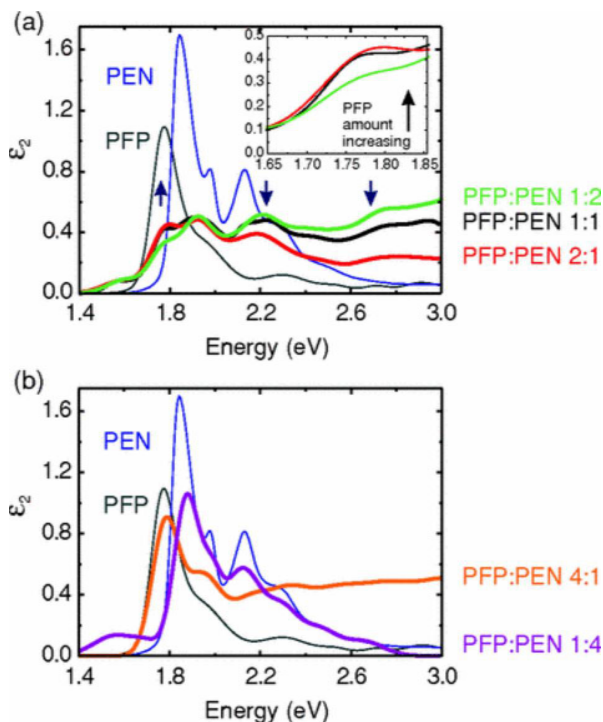


**FIG. 9.** Optical properties in PEN:PPF blends, forming co-crystals. An additional absorption band occurs below the optical bandgap of the neat compounds at 1.6 eV that can be attributed to the formation of an ordered complex. See text for details. Reprinted with permission from Broch *et al.*, *Phys. Rev. B* **83**, 245307 (2011). Copyright 2011 American Physical Society.<sup>61</sup>

ratio.<sup>186</sup> This stabilized ordered structure is thus also expected to be realized in PEN:PPF blends deviating from the equimolar mixing ratio.

#### D. Phase separation in co-crystal blends

Figure 8 further contains GIXD scans for PEN:PPF blends with an excess of one molecular compound. Compared to the equimolar blend, the same diffraction peaks are visible (A–F), but in addition, Bragg peaks corresponding to the excess pristine phase are observed (indicated by their Miller indices).<sup>62</sup> Therefore, the co-crystal phase separates from the pure phase of the excess compound, resulting in a superposition of the two in the x-ray diffractograms. It should be noted that the two phases can interfere with each other, giving rise to minor shifts in Bragg peak positions.<sup>62</sup>

Optical absorption spectra for non-equimolar PEN:PPF blends are shown in Fig. 9. Especially for the more extreme mixing ratios presented in Fig. 9(b), it becomes obvious that their absorption spectra cannot be explained by a superposition of the absorption spectra of the neat compounds and the equimolar blend. Thus, either surface effects at grain boundaries or differences in molecular composition (mixing ratio) in the neat and the equimolar, co-crystalline phases might possibly cause changes to the optical response.

For PEN:PPF blends, the formation of a co-crystal mainly has been motivated above by their similarity in molecular geometry and

the inverted quadrupole moment upon perfluorination. The molecular orbital alignment between the two molecules results in molecular orbital hybridization by formation of a charge-transfer complex. In general, charge-transfer complex formation seems to be a strong driving force for the formation of an ordered co-crystal.<sup>77</sup> The formation of charge-transfer complexes also has been reported for other binary systems containing PEN.<sup>60,194,195</sup> There, F4-TCNQ and F6-TCNNQ have been used as strong molecular acceptor molecules. These two molecules are commonly used as p-type molecular dopants.<sup>51</sup> Note, however, that sophisticated alternative approaches for the efficient doping of organic semiconductors are developed, for example, by making use of organic salts and photocatalysts.<sup>20</sup> Especially for F6-TCNNQ, its energetically favorable electron affinity results in the formation of ion pairs if mixed with PEN, while for F4-TCNQ, both ion pair formation and hybridization in a charge-transfer complex with PEN are observed.<sup>60</sup> The Coulombic energy between the obtained PEN cation and acceptor anion is highly attractive. However, in stark contrast to the PEN:PPF system, for which the molecular dimensions agree, PEN and F6-TCNNQ are geometrically non-compatible. Therefore, no long-range crystalline ordering, but instead an amorphous mixed phase with solely short-range order, is obtained.<sup>19</sup> In blends containing an excess of PEN, this amorphous phase separates from the pristine PEN phase. The latter is polycrystalline and randomly oriented, induced by the amorphous and, therefore, isotropic, mixed phase.

#### VII. COMPLEX OR INTERMEDIATE MIXING REGIMES

The binary mixtures discussed above are excellent examples to illustrate the three general mixing scenarios, namely, formation of a solid solution, phase separation, and co-crystal formation. However, as can be concluded from the idealized potential energy surfaces shown in Fig. 1, intermediate scenarios can also be envisaged. For example, phase separation only within a limited range of mixing scenarios is possible. Furthermore, the separated phases might still contain both molecular species but with different concentrations, thus representing a system with two partially mixed phases. These scenarios will be illustrated next using binary blends of PEN with 5PH and PEN with 3P. The former illustrates that mixing can change with thin-film thickness as concluded from XRD data, while in the latter, focus is given to the optical properties for a system that phase separates into two partially mixed phases. It is important to realize that these more intricate scenarios will naturally depend more sensitively on changes of the preparation parameters, such as substrate temperature, deposition rate, and nature of the substrate.

##### A. Thickness-dependent mixing

PEN mixed with 5PH has been shown to be an organic binary system for which the mixing behavior depends on the film thickness.<sup>64</sup> Furthermore, it is said to undergo limited intermixing.<sup>63,64</sup> This term describes the observation that a single mixed phase forms for mixing ratios with an excess of PEN molecules down to approximately the equimolar mixing ratio, but an additional pure 5PH phase separates for an excess of 5PH in the blends. Thus, Bragg reflections at  $q$ -values identical to pure 5PH and diffraction peaks at  $q$ -values intermediate to neat PEN and 5PH are observed in these 5PH-rich mixtures, as illustrated in Fig. 10. This can be concluded, for example, from the (002) Bragg peak (red circle) in the XRR diffractogram for

the PEN:5PH 1:4 mixture (blue curve), for which an additional peak in the shoulder at higher  $q$ -values is discernible that coincides with the (002) Bragg peak for neat 5PH. A similar doublet is also observable for the (21L) peak in the GIXD data [Fig. 10(b)]. Note, however, that in contrast to the XRR data, the larger in-plane dimension of 5PH compared to PEN (Table I) lets the Bragg peak of phase-separated neat 5PH appear at lower  $q$ -values to the Bragg peak that corresponds to the mixed phase.

The observation of limited intermixing only for an excess of 5PH has been attributed to the minor differences in molecular size.<sup>63</sup> It is easier to dissolve the shorter 5PH molecule in a lattice of longer PEN than vice versa. Therefore, the formation of a phase of higher PEN concentration by phase separation of a neat 5PH phase might be beneficial for reducing the free energy by releasing stress.<sup>63,64</sup> However, this argument only holds for the changes in molecular dimension along the long molecular axis, but the largest differences between the two molecular compounds are observed for the short axis of the molecular planes (see Table I). Along the short molecular axis, 5PH acts as the larger of the two molecules. Thus, despite the fact that PEN and 5PH exhibit the most pronounced disparities in molecular dimensions among the rod-like molecules addressed in this paper, the aforementioned argument is unable to provide a definitive explanation for the observation of limited intermixing in this system. In addition, no indication for phase separation has been observed for PEN co-deposited with TET, despite the even larger absolute differences along the long molecular dimension.<sup>24</sup> Only for alternate deposition of the two materials, clear signatures of phase separation have been observed.<sup>196</sup> Therefore, while structural compatibility is a significant factor in understanding mixing behavior, it is not the sole determinant. Additional considerations must be taken into account to gain a comprehensive understanding of this phenomenon.

Depth-dependent GIXD measurements through variation in the grazing incident angle for PEN:5PH blends with an excess of 5PH have demonstrated that the mixing behavior in the system depends on the sample thickness.<sup>64</sup> The variation in the incident angle alters the penetration depth of the evanescent wave into the organic film, thus allowing for sensitivity to surface and bulk structures within the organic layer. This thickness-dependent mixing behavior has been further confirmed by real-time GIXD experiments that showed that phase separation in this system starts from the second monolayer.<sup>64</sup> From these and related observations in other binary systems, it can be concluded that differences in the thin-film growth modes of the two molecular compounds are important in determining the mixing scenario.<sup>90</sup> While PEN grows in a Stranski–Krastanov mode with closed layers at the initial stage of thin-film growth,<sup>147</sup> for 5PH, an immediate island formation corresponding to the Volmer–Weber growth mode has been reported.<sup>197,198</sup> This indicates that newly arriving 5PH molecules that encounter clusters of 5PH molecules during thin-film growth show a tendency for interlayer diffusion to upper layers, separating from the PEN:5PH mixed phase in molecular layers closer to the substrate surface. PEN, on the other hand, tends to wet the surface, thus preferably accumulating in layers closer to the substrate. It might be interesting to perform deposition experiments under a glancing angle to elaborate on this hypothesis.<sup>100</sup>

Importantly, the tendency for island formation might change in the blends compared to the neat compounds, as can be concluded from changes in the morphology for blended films (see, e.g., Ref. 63).

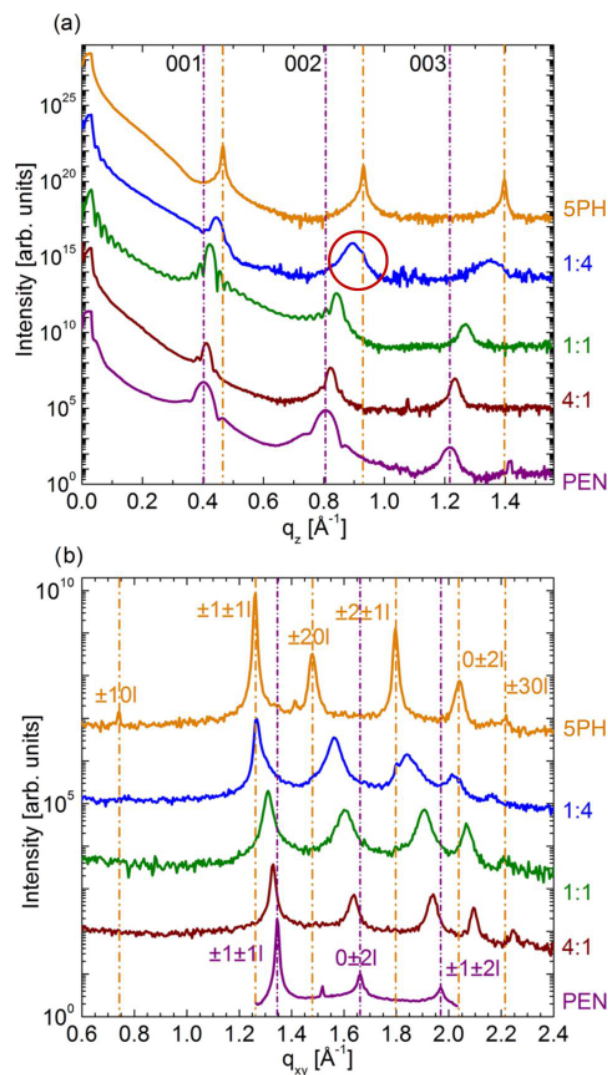


**FIG. 10.** XRD for PEN:5PH mixtures of various mixing ratios in (a) XRR and (b) GIXD geometry. Phase separation into a pure 5PH and a mixed phase can be concluded from the doublet in Bragg peaks in the 1:4 (PEN:5PH) blend (blue curves). Bragg peak positions for pure 5PH are indicated by vertical yellow lines. Vertical purple lines correspond to Bragg peak positions for pure PEN. Adapted with permission from Dieterle *et al.*, *J. Phys. Chem. C* **119**(47), 26339–26347 (2015). Copyright 2015 American Chemical Society.<sup>63</sup>

This can be rationalized by the fact that the growth mode depends, *inter alia*, on the interplay of molecule–molecule and molecule–substrate interaction.<sup>198,199</sup> With the presence of the secondary molecular compound in the binary blends, additional heteromolecular interaction occurs. Furthermore, the slight changes in molecular size of the two compounds also cause changes in the orientation of the molecules at the grain boundaries, thus altering the distribution of Ehrlich–Schwöbel barriers that has an impact on the growth mode.<sup>200</sup>

The observation of phase separation and, in particular, limited intermixing by XRD techniques requires the presence of significant

amounts of the two or more phases in the sample with pronounced scattering intensity. Especially for blends of structurally similar molecules, differences in Bragg peak positions are rather small, and thus the formation of a solid solution, phase separation, and limited intermixing might be challenging to discern. Thus, complementary approaches are required that allow for a closer inspection of the mixing behavior. An example is optical absorption spectroscopy, which probes the mixing behavior on a smaller length scale compared to XRD by being sensitive to the intermolecular interaction. For PEN:5PH blends, this has been done by probing the absorption spectrum for 5PH:PEN-host:guest blends in the doping regime.<sup>201</sup> Interestingly, spectral differences between electronically coupled and decoupled PEN molecules have been observed. Thus, even in what has been proposed as the phase-separated neat 5PH phase in Refs. 63 and 64, there might be small amounts of PEN molecules dissolved. This would be consistent with the thermodynamic interpretation presented in Eq. (1) and Fig. 1 that showed that entropy is a strong driving force that ensures mixing at doping concentrations. We elaborate on the investigation of the mixing behavior for intermediate mixing scenarios using optical spectroscopy techniques by taking a closer look at the UV/vis absorption spectra in binary blends of PEN with 3P.

At this point, we would like to stress that additional techniques for probing the mixing behavior by measuring the intermolecular interaction exist. For example, in Ref. 202, statistical intermixing in binary blends has been concluded from the breakdown of a splitting in infrared active vibrations whose origin in the solid state has been proposed as being attributable to Davydov splitting between translationally inequivalent molecules. However, the energy of vibrational bands is even more strongly defined by the single-molecule properties compared to UV/vis absorption spectroscopy; thus, this alternative technique might only be suitable for some specific systems.

## B. Partial phase separation

The intricacies of phase separation into partially mixed phases and the strength of optical spectroscopy techniques for their observation and investigation are demonstrated by binary blends of PEN and 3P. This material combination has received great interest in the past for studying the single-molecule properties of PEN as a guest molecule in a host lattice of 3P molecules.<sup>203–208</sup> This is in part motivated by the large optical bandgap of 3P that allows for clear and unambiguous assignment of the low-energy absorption properties to originate from PEN. In contrast to the numerous reports of 3P:PEN mixtures in host-guest systems, only a limited number of reports exist that focused on the mixing behavior of PEN and 3P at intermediate mixing ratios.<sup>70,173,209</sup> The latter experiments were mainly motivated by investigations of singlet exciton fission in PEN using electron paramagnetic resonance spectroscopy.<sup>70</sup> In the literature, the formation of a solid solution with no evidence of phase separation has been inferred from x-ray diffraction analysis.<sup>70,173</sup> However, distinct differences compared to the optical properties of solid solutions as detailed above are observed. This will be discussed in the following.

In Fig. 11(a), room-temperature optical absorption spectra for PEN:3P blends are shown that qualitatively match literature reports.<sup>70</sup> Namely, in addition to two low-energy absorption bands that have been attributed to the Davydov components, a rather sharp absorption band at 2.1 eV (590 nm, dashed line in Fig. 11) is visible,

especially for smaller PEN concentrations ( $\leq 25\%$ ). Based on a comparison with optical absorption spectra for highly diluted PEN, the latter band can be safely assigned to the optical bandgap of isolated, electronically decoupled PEN embedded in a 3P host matrix.<sup>70</sup> Such an additional sharp absorption band has not been observed at intermediate mixing ratios differing from the doping regime for any of the solid solutions discussed above. Furthermore, apart from an obvious decrease in overall absorbance for decreasing PEN concentration, neither the spectral shape nor the energetic position of the Davydov components (at 1.92 and 2.03 eV) changes with mixing ratio. To unravel this divergent behavior in optical properties from the solid solutions discussed above, we performed temperature-dependent UV/vis measurements in the temperature range from 300 K down to 80 K in increments of 20 K (Fig. 11). Lowering the temperature serves to reduce thermal broadening in the optical absorption spectra, thus enabling discrimination of closely separated absorption bands.

As can be seen in the absorption spectra of the mixed thin films recorded at 80 K in Fig. 11(b), Davydov splitting in PEN:3P manifests in at least three absorption bands (see the solid vertical bars), all of which are distinctly different from the optical properties of electronically decoupled PEN (dashed vertical bar). Thus, they must be the result of some form of electronic coupling to neighboring molecules. Note that our experimental data do not allow discrimination of electronic coupling between PEN molecules only, or between PEN and 3P. Importantly, an assignment to the lower and upper Davydov components in PEN becomes no longer feasible. However, based on the robustness of the energetic position of the optical absorption bands with mixing ratio, which is likewise the case for PEN in phase-separating mixtures as discussed above, we propose that PEN and 3P separate into partially mixed phases. Future experiments at lower deposition rates or with interrupted growth may allow elaboration of this hypothesis by modifying the interplay between thermodynamic and kinetic aspects of thin-film growth.<sup>98,99</sup> Both approaches would lower the impact of kinetics on the mixing behavior, thus potentially facilitating the observation of phase separation also by the XRD technique. Therefore, binary blends of PEN and 3P have the potential to provide new insights into the interplay between thermodynamic and kinetic aspects in the mixing of organic binary thin films prepared by OMBD.

Alternatively, the higher number of low-energy absorption bands in PEN:3P blends compared to PEN in solid solutions could be the result of a possible phase transition upon cooling down the samples. In particular, 3P is known to undergo a phase transition at about 191 K from a monoclinic unit cell containing two conformationally disordered molecules at higher temperatures to a triclinic unit cell containing eight conformationally ordered molecules.<sup>55,150,164</sup> However, no indication of a phase transition is visible in the temperature-dependent UV/vis absorption spectra of the 50% PEN:50% 3P blend shown in Fig. 11(c). Instead, changes in absorption bands build up continuously. Nevertheless, this does not rule out the existence of a phase transition also in the binary mixtures, but UV/vis spectroscopy is not capable of resolving it, thus demanding alternative detection techniques.<sup>183</sup> For example, for 3P:TET host-guest systems, the phase transition has been observed using Raman spectroscopy, a technique that is highly sensitive to the single molecule.<sup>55</sup>

In Fig. 11(d), difference absorption spectra [absorbance( $T$ ,  $\lambda$ ) - absorbance( $T = 280$  K,  $\lambda$ )] for the 50% PEN:50% 3P sample are

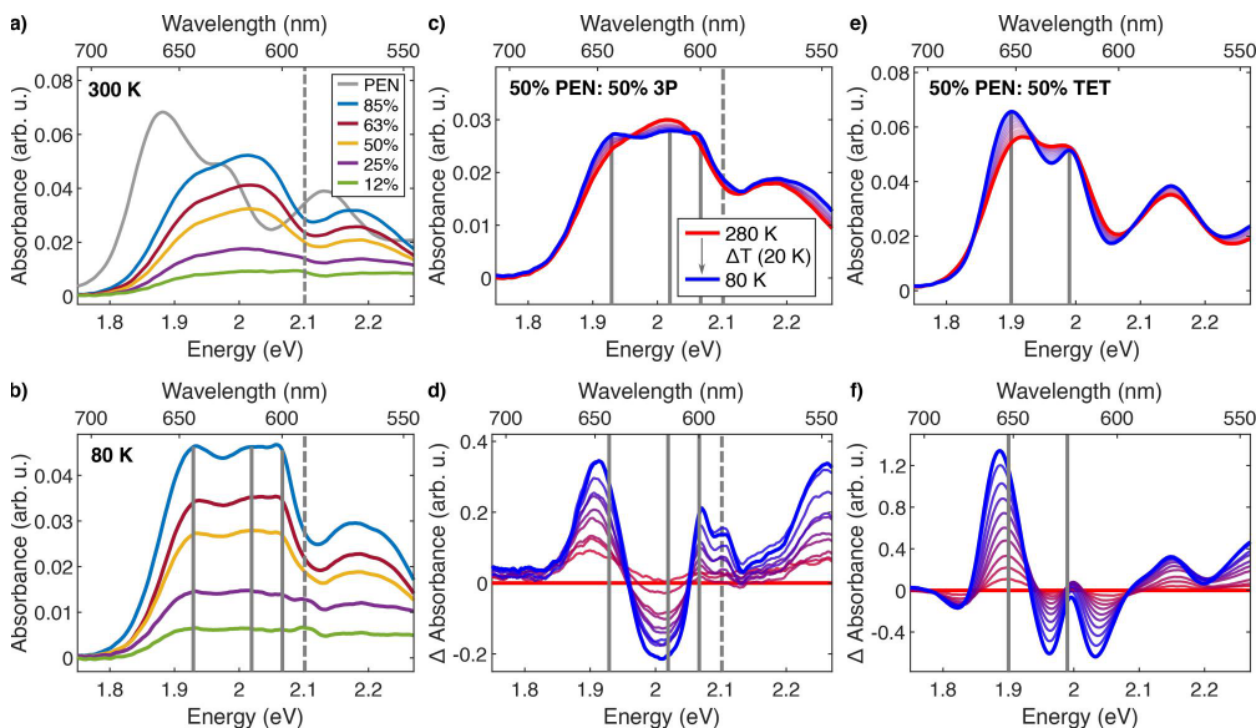


**FIG. 11.** Temperature-dependent optical properties in binary mixtures containing PEN. (a) and (b) Absorption spectra for PEN:3P blends at 300 and 80 K, respectively. (c) and (e) Temperature-dependent absorption spectra for 50% PEN:50% 3P and 50% PEN:50% TET, respectively. (d) and (f) Absorption difference spectra for the data shown in (c) and (e). As a reference, the spectrum at 280 K (red baseline) has been used. The dashed vertical line corresponds to the reported absorption band of isolated PEN in 3P at 590 nm.<sup>70</sup> Solid vertical lines for orientation.

shown. Interestingly, in addition to the three low-energy absorption bands, these spectra further allow for the discrimination of an additional evolving signature at 2.1 eV that matches in energy with the optical properties of isolated PEN in a matrix of 3P.<sup>70</sup> This indicates that a significant amount of electronically decoupled PEN is present even in the 50% PEN:50% 3P mixture. Furthermore, it confirms the electronically coupled origin of all lower-energy absorption bands, a requirement for a classification as an organic molecular alloy.<sup>174</sup>

For comparison, we further investigated temperature-dependent absorption spectra for PEN:TET solid solutions [Figs. 11(e) and 11(f)]. In contrast to the 50% PEN:50% 3P sample, Davydov splitting in PEN:TET blends is always composed of two components only, with no observation of additional absorption bands upon lowering the temperature. Apart from a minor shift in the energetic position, especially for the lower Davydov component and in agreement with literature,<sup>57,210,211</sup> lowering the temperature in the 50% PEN:50% TET sample narrows the width of absorption bands. Thus, the two Davydov components, which partially overlap at room temperature, become distinguishable more easily at cryogenic temperatures.

Interestingly, from the difference absorption spectra shown in Fig. 11(f), a weak absorption band can be speculated to exist at an energy of 2.1 eV. The electronic nature of this weak absorption band, which is hidden behind the absorption band at 2.15 eV that has been shown to be the result of a combination of optical transitions to charge-transfer electronic and vibronic states,<sup>24</sup> is unclear so far.

While it could be of a charge-transfer nature, it is also possible that it is the result of electronically decoupled PEN. Furthermore, it is possible that it actually corresponds to Davydov splitting in the first vibronic progression. In agreement with the literature, this splitting in the first vibronic progression would be smaller compared to Davydov splitting without vibrational quanta, both in the classical picture with Coulomb-type coupling only and by inclusion of coupling to charge-transfer states.<sup>26,127,212,213</sup>

## VIII. SUMMARY AND FUTURE DIRECTIONS

The purpose of the paper was to highlight the differences in the structural and optical properties of binary blends containing PEN but differing in their mixing behavior due to the choice of the second molecular compound. Three general mixing scenarios exist, namely, the formation of a solid solution, phase separation, and co-crystal formation.

The formation of a solid solution, with a statistical occupation of lattice sites, requires structural similarity of the molecules as a necessary prerequisite. Furthermore, the intermolecular interactions between like and dissimilar molecules should be comparable. Additionally, isomorphism and identical thin-film growth modes support the formation of a solid solution. In solid solutions, the crystal lattice parameters change continuously between the ones obtained for the pure compounds. Deviations from a strictly linear trend in the lattice parameters are the result of weak van der Waals intermolecular

interactions typically present in organic semiconductor crystals. Therefore, the shallow minima in the potential energy surface<sup>80</sup> facilitate slight adaptations in molecular orientation to minimize the total free energy. A continuous change is also observed for the optical absorption properties of PEN in solid solutions. For decreasing PEN concentration, a decrease in Davydov splitting is observed, which can be understood as a decrease in charge-transfer admixture to the Davydov components due to the induced structural disorder.<sup>24,58,128</sup> Depending on the choice of the second molecular species, differently pronounced shifts in the energetic position of the optical transitions can be induced. Empirically, stronger shifts are observed for molecules of larger optical bandgap.

Phase separation takes place in particular for organic binary blends containing structurally dissimilar molecules. The positions of the Bragg peaks remain robust, independent of the molar fraction, although minor changes are possible via interference effects.<sup>62</sup> Likewise, no clear shifts in PEN optical absorption bands are observed, and also the relative peak intensities are mainly preserved. However, mixing of structurally dissimilar molecules leads to a breakdown of the long-range structural order. Therefore, the uniaxial orientation of PEN molecules is lifted in PEN:C<sub>60</sub> blends, strongly reducing the intensity of Bragg reflections in specular geometry, corresponding to the out-of-plane lattice spacing. Furthermore, the induced random orientation of crystallites in this system reduces the absorption intensity of PEN for illumination under normal incidence. Such a loss in crystalline order might be responsible for the reported reduction in solar cell performance, although chemical bonding between PEN and C<sub>60</sub> molecules likely plays a role as well.

Ordered co-crystals are obtained for strongly attractive intermolecular interactions between structurally congruent molecules. New diffraction peaks are observed that cannot be explained by the crystal structures of the neat compounds. As these molecules compose an ordered alternating superstructure, phase separation is observed for mixing ratios differing from the equimolar one. Therein, the co-crystal separates from the pristine phase of the excess molecular compound. The strong intermolecular interaction of the two molecules frequently leads to the observation of new bands in their optical absorption spectra. These can be either due to electronic transitions from intermolecular hybrid orbitals in the case of charge-transfer complex formation or from electronic transitions of ionized molecules in the case of ion pair formation. However, the absence of any new absorption features is no proof of a lack of formation of an ordered crystal.

Thus, while not being the primary focus of this work, computational approaches are essential for a comprehensive understanding of the optical properties of such systems. In particular, they can help disentangle the contributions of different electronic states and vibronic couplings underlying the observed absorption features. However, these approaches remain challenging due to their high computational cost and the need for approximations. The complexity arises from the simultaneous relevance of multiple electronic states (Frenkel, charge resonance, and charge transfer) and low- and high-frequency vibrational modes, as well as static and dynamic disorder.<sup>24,26,124,214</sup> Nevertheless, several promising computational strategies have been recently developed that successfully address multicomponent organic systems, paving the way for a more complete understanding of their complex optical behavior (see, e.g., Refs. 24, 142, 215, and 216).

It should be kept in mind that the three general mixing scenarios in binary blends are extreme cases. Intermixture caused by entropy dominates, especially for limiting mixing concentrations close to the pure compounds. Therefore, doping is almost always possible, while for mixing ratios closer to the equimolar one, separation into two partially mixed phases becomes more likely. Thin-film growth by OMBD is a non-equilibrium process, thus facilitating shifting the boundary between mixing and demixing through kinetic control. Unraveling the intricacies of the interplay between thermodynamically and kinetically controlled mixing behavior on a fundamental level is of particular interest for the application of organic binary mixtures in optoelectronic devices.

A suitable candidate to investigate that is the PEN:3P system, for which we observe the separation into two partially mixed phases upon preparation of thin films via OMBD. Adjusting the deposition rate and substrate temperature possibly allows for switching between different mixing behaviors. A thorough experimental investigation in combination with computational simulations would deepen our understanding of the mixing behavior in organic binary systems on a nanoscopic, molecular level. In the same context, long-term stability of kinetically trapped binary mixtures is of interest, especially for applications.

Although limited to blends containing PEN as one of the two molecular compounds, this paper illustrates the relationship between structural and optical properties in mixed binary systems. By appropriate combination of the molecular compounds, optimization of optical, electronic, and optoelectronic devices based on small organic molecules becomes accessible. Thin-film growth as a non-equilibrium process possible allows for altering the mixing behavior and/or morphology within limits through kinetically controlled growth.<sup>98–100,173</sup>

So far, research has mainly focused on binary organic mixed blends, with only rare cases extending the complexity by the inclusion of additional compounds.<sup>1,53,217,218</sup> Profound fundamental knowledge on binary systems is key to understand and fully exploit the potential of these higher systems. Thus, this paper lays the foundations for a better understanding of ternary blends and paves the road for organic high-entropy alloys.

## ACKNOWLEDGMENTS

Financial support from the German Research Foundation (BR4869/4-1 and SCHR700/40-1) is gratefully acknowledged. We also thank in particular Katharina Broch, Alexander Gerlach, Alexander Hinderhofer, and Sara Haug for their discussions and contributions in the early stages of the project as well as numerous collaborators for insightful discussions.

## AUTHOR DECLARATIONS

### Conflict of Interest

The authors have no conflicts to disclose.

## Author Contributions

**Frederik Unger:** Conceptualization (supporting); Data curation (lead); Formal analysis (equal); Methodology (equal); Project administration (equal); Software (equal); Validation (equal); Visualization (lead); Writing – original draft (lead); Writing – review & editing

(equal). **Frank Schreiber**: Conceptualization (lead); Funding acquisition (lead); Methodology (equal); Project administration (equal); Resources (lead); Supervision (lead); Validation (equal); Visualization (supporting); Writing – original draft (supporting); Writing – review & editing (equal).

## DATA AVAILABILITY

The data that support the findings of this study are available from the corresponding author upon reasonable request.

## APPENDIX: EXPERIMENTAL METHODS

While experimental data for most of the systems discussed in the manuscript have already been published,<sup>13,24,25,58–68</sup> here, the experimental methods for the additionally prepared thin film blends of PEN (Sigma-Aldrich, 99.99%, triple sublimed) and 3P (Sigma-Aldrich,  $\geq 99.5\%$ ) using OMBD at a base pressure of  $5 \times 10^{-8}$  mbar are presented. The substrate temperature was set to  $-15^\circ\text{C}$  (258 K) to account for the low sticking coefficient and challenges associated with the growth of 3P.<sup>173</sup> Note, however, that at such lower substrate temperatures, 3P molecules, present in the chamber due to its high vapor pressure, begin to adsorb on the substrate. The thin films with a nominal thickness of 20 nm were grown at a growth rate of 0.6 nm/min on fused silica glass substrates (JGS1, Microchemicals). The growth rates of the two molecular compounds were monitored individually by two quartz crystal microbalances (QCMs).

Optical UV/vis absorption spectra were measured using a Perkin Elmer Lambda 950 spectrophotometer. For temperature-dependent UV/vis absorption measurements, the samples were mounted on a cryostat (OptistatCF-V, Oxford Instruments). The cryostat was constantly cooled by liquid nitrogen, and the temperature was controlled by resistive heating. Samples were measured in the temperature range from room temperature down to 80 K in steps of 20 K. A minimum of 10 min was allowed for the temperature of the substrate to stabilize before measurement at a given temperature.

## REFERENCES

- <sup>1</sup>N. Gasparini, A. Salleo, I. McCulloch, and D. Baran, “The role of the third component in ternary organic solar cells,” *Nat. Rev. Mater.* **4**, 229–242 (2019).
- <sup>2</sup>N. Li, J. D. Perea, T. Kassar, M. Richter, T. Heumueller, G. J. Matt, Y. Hou, N. S. Güldal, H. Chen, S. Chen, S. Langner, M. Berlinghof, T. Unruh, and C. J. Brabec, “Abnormal strong burn-in degradation of highly efficient polymer solar cells caused by spinodal donor-acceptor demixing,” *Nat. Commun.* **8**, 14541 (2017).
- <sup>3</sup>R. Fitzner, E. Mena-Osteritz, A. Mishra, G. Schulz, E. Reinold, M. Weil, C. Körner, H. Ziehlke, C. Elschner, K. Leo, M. Riede, M. Pfeiffer, C. Uhrich, and P. Bäuerle, “Correlation of  $\pi$ -conjugated oligomer structure with film morphology and organic solar cell performance,” *J. Am. Chem. Soc.* **134**, 11064–11067 (2012).
- <sup>4</sup>J.-L. Brédas, J. E. Norton, J. Cornil, and V. Coropceanu, “Molecular understanding of organic solar cells: The challenges,” *Acc. Chem. Res.* **42**, 1691–1699 (2009).
- <sup>5</sup>B. A. Gregg, “The photoconversion mechanism of excitonic solar cells,” *MRS Bull.* **30**, 20–22 (2005).
- <sup>6</sup>A. Wadsworth, Z. Hamid, J. Kosco, N. Gasparini, and I. McCulloch, “The bulk heterojunction in organic photovoltaic, photodetector, and photocatalytic applications,” *Adv. Mater.* **32**, 2001763 (2020).
- <sup>7</sup>J. Wagner, M. Gruber, A. Hinderhofer, A. Wilke, B. Bröker, J. Frisch, P. Amsalem, A. Vollmer, A. Opitz, N. Koch, F. Schreiber, and W. Brütting, “High fill factor and open circuit voltage in organic photovoltaic cells with diindenoperylene as donor material,” *Adv. Funct. Mater.* **20**, 4295–4303 (2010).
- <sup>8</sup>M. Fahlman, S. Fabiano, V. Gueskine, D. Simon, M. Berggren, and X. Crispin, “Interfaces in organic electronics,” *Nat. Rev. Mater.* **4**, 627–650 (2019).
- <sup>9</sup>Z. Qin, C. Gao, W. W. H. Wong, M. K. Riede, T. Wang, H. Dong, Y. Zhen, and W. Hu, “Molecular doped organic semiconductor crystals for optoelectronic device applications,” *J. Mater. Chem. C* **8**, 14996–15008 (2020).
- <sup>10</sup>M. Lusi, “Engineering crystal properties through solid solutions,” *Crystr. Growth Des.* **18**, 3704–3712 (2018).
- <sup>11</sup>J.-H. Dou, Z.-A. Yu, J. Zhang, Y.-Q. Zheng, Z.-F. Yao, Z. Tu, X. Wang, S. Huang, C. Liu, J. Sun, Y. Yi, X. Cao, Y. Gao, J.-Y. Wang, and J. Pei, “Organic semiconducting alloys with tunable energy levels,” *J. Am. Chem. Soc.* **141**, 6561–6568 (2019).
- <sup>12</sup>M. Schwarze, W. Tress, B. Beyer, F. Gao, R. Scholz, C. Poelking, K. Ortstein, A. A. Günther, D. Kasemann, D. Andrienko, and K. Leo, “Band structure engineering in organic semiconductors,” *Science* **352**, 1446–1449 (2016).
- <sup>13</sup>F. Unger, L. Moretti, J. Hausch, J. Bredehoeft, C. Zeiser, S. Haug, R. Tempelaar, N. J. Hestand, G. Cerullo, and K. Broch, “Modulating singlet fission by scanning through vibronic resonances in pentacene-based blends,” *J. Am. Chem. Soc.* **144**(45), 20610–20619 (2022).
- <sup>14</sup>M. Morimoto, S. Kobatake, and M. Irie, “Multicolor photochromism of two- and three-component diarylethene crystals,” *J. Am. Chem. Soc.* **125**, 11080–11087 (2003).
- <sup>15</sup>C.-H. Wang, S.-D. Jian, S.-W. Chan, C.-S. Ku, P.-Y. Huang, M.-C. Chen, and Y.-W. Yang, “Enhanced stability of organic field-effect transistors with blend pentacene/anthradithiophene films,” *J. Phys. Chem. C* **116**, 1225–1231 (2012).
- <sup>16</sup>G. Campillo-Alvarado, M. Bernhardt, D. W. Davies, J. A. N. T. Soares, T. J. Woods, and Y. Diao, “Modulation of  $\pi$ -stacking modes and photophysical properties of an organic semiconductor through isosteric cocrystallization,” *J. Chem. Phys.* **155**, 071102 (2021).
- <sup>17</sup>D. Konarev, R. Lyubovskaya, N. Drichko, V. Semkin, and A. Graja, “Energies of charge transfer for  $C_{60}$  and  $C_{70}$  complexes in solutions and in the solid state,” *Chem. Phys. Lett.* **314**, 570–576 (1999).
- <sup>18</sup>P. Yu, Y. Zhen, H. Dong, and W. Hu, “Crystal engineering of organic optoelectronic materials,” *Chem* **5**, 2814–2853 (2019).
- <sup>19</sup>H. Kleemann, C. Schuenemann, A. A. Zakhidov, M. Riede, B. Lüssem, and K. Leo, “Structural phase transition in pentacene caused by molecular doping and its effect on charge carrier mobility,” *Org. Electron.* **13**, 58–65 (2012).
- <sup>20</sup>W. Jin, C.-Y. Yang, R. Pau, Q. Wang, E. K. Tekelenburg, H.-Y. Wu, Z. Wu, S. Y. Jeong, F. Pitzalis, T. Liu, Q. He, Q. Li, J.-D. Huang, R. Kroon, M. Heeney, H. Y. Woo, A. Mura, A. Motta, A. Facchetti, M. Fahlman, M. A. Loi, and S. Fabiano, “Photocatalytic doping of organic semiconductors,” *Nature* **630**, 96–101 (2024).
- <sup>21</sup>M. Gruber, M. Rawolle, J. Wagner, D. Magerl, U. Hörmann, J. Perlich, S. V. Roth, A. Opitz, F. Schreiber, P. Müller-Buschbaum, and W. Brütting, “Correlating structure and morphology to device performance of molecular organic donor–acceptor photovoltaic cells based on diindenoperylene (DIP) and  $C_{60}$ ,” *Adv. Energy Mater.* **3**, 1075–1083 (2013).
- <sup>22</sup>A. Opitz, J. Wagner, W. Brütting, A. Hinderhofer, and F. Schreiber, “Molecular semiconductor blends: Microstructure, charge carrier transport, and application in photovoltaic cells,” *Phys. Status Solidi A* **206**, 2683–2694 (2009).
- <sup>23</sup>H. Zhao, C. E. Arneson, D. Fan, and S. R. Forrest, “Stable blue phosphorescent organic LEDs that use polariton-enhanced Purcell effects,” *Nature* **626**, 300–305 (2024).
- <sup>24</sup>F. Unger, D. Lepple, M. Asbach, L. Craciunescu, C. Zeiser, A. F. Kandolf, Z. Fišer, J. Hagara, J. Hagenlocher, S. Hiller, S. Haug, M. Deutsch, P. Grüniger, J. Novák, H. F. Bettinger, K. Broch, B. Engels, and F. Schreiber, “Optical absorption properties in pentacene/tetracene solid solutions,” *J. Phys. Chem. A* **128**(4), 747–760 (2024).
- <sup>25</sup>A. Hinderhofer, J. Hagenlocher, A. Gerlach, J. Krug, M. Oettel, and F. Schreiber, “Nonequilibrium roughness evolution of small molecule mixed

- films reflecting equilibrium phase behavior," *J. Phys. Chem. C* **126**, 11348–11357 (2022).
- <sup>26</sup>N. J. Hestand and F. C. Spano, "Expanded theory of H- and J-molecular aggregates: The effects of vibronic coupling and intermolecular charge transfer," *Chem. Rev.* **118**, 7069–7163 (2018).
- <sup>27</sup>G. K. R. Senadeera, P. V. V. Jayaweera, V. P. S. Perera, and K. Tennakone, "Solid-state dye-sensitized photocell based on pentacene as a hole collector," *Sol. Energy Mater.* **73**, 103–108 (2002).
- <sup>28</sup>N. E. Gruhn, D. A. da Silva Filho, T. G. Bill, M. Malagoli, V. Coropceanu, A. Kahn, and J.-L. Brédas, "The vibrational reorganization energy in pentacene: Molecular influences on charge transport," *J. Am. Chem. Soc.* **124**, 7918–7919 (2002).
- <sup>29</sup>C. Dimitrakopoulos and P. Malenfant, "Organic thin film transistors for large area electronics," *Adv. Mater.* **14**, 99–117 (2002).
- <sup>30</sup>J. E. Anthony, "The larger acenes: Versatile organic semiconductors," *Angew. Chem., Int. Ed.* **47**, 452–483 (2008).
- <sup>31</sup>T. Minakata, H. Imai, and M. Ozaki, "Electrical properties of highly ordered and amorphous thin films of pentacene doped with iodine," *J. Appl. Phys.* **72**, 4178–4182 (1992).
- <sup>32</sup>A. Ashoka, N. Gauriot, A. V. Girija, N. Sawhney, A. J. Sneyd, K. Watanabe, T. Taniguchi, J. Sung, C. Schnedermann, and A. Rao, "Direct observation of ultrafast singlet exciton fission in three dimensions," *Nat. Commun.* **13**, 5963 (2022).
- <sup>33</sup>C. Jundt, G. Klein, B. Sipp, J. Le Moigne, M. Joucla, and A. Villaeys, "Exciton dynamics in pentacene thin films studied by pump-probe spectroscopy," *Chem. Phys. Lett.* **241**, 84–88 (1995).
- <sup>34</sup>M. W. B. Wilson, A. Rao, J. Clark, R. S. S. Kumar, D. Brida, G. Cerullo, and R. H. Friend, "Ultrafast dynamics of exciton fission in polycrystalline pentacene," *J. Am. Chem. Soc.* **133**, 11830–11833 (2011).
- <sup>35</sup>J. Burgos, M. Pope, C. E. Swenberg, and R. R. Alfano, "Heterofission in pentacene-doped tetracene single crystals," *Phys. Status Solidi B* **83**, 249–256 (1977).
- <sup>36</sup>D. Knipp, R. A. Street, and A. R. Völkel, "Morphology and electronic transport of polycrystalline pentacene thin-film transistors," *Appl. Phys. Lett.* **82**, 3907–3909 (2003).
- <sup>37</sup>M. C. Hanna and A. J. Nozik, "Solar conversion efficiency of photovoltaic and photoelectrolysis cells with carrier multiplication absorbers," *J. Appl. Phys.* **100**, 074510 (2006).
- <sup>38</sup>A. Rao and R. H. Friend, "Harnessing singlet exciton fission to break the Shockley–Queisser limit," *Nat. Rev. Mater.* **2**, 17063 (2017).
- <sup>39</sup>P. J. Jadhav, A. Mohanty, J. Sussman, J. Lee, and M. A. Baldo, "Singlet exciton fission in nanostructured organic solar cells," *Nano Lett.* **11**, 1495–1498 (2011).
- <sup>40</sup>N. J. Thompson, D. N. Congreve, D. Goldberg, V. M. Menon, and M. A. Baldo, "Slow light enhanced singlet exciton fission solar cells with a 126% yield of electrons per photon," *Appl. Phys. Lett.* **103**, 263302 (2013).
- <sup>41</sup>D. N. Congreve, J. Lee, N. J. Thompson, E. Hontz, S. R. Yost, P. D. Reusswig, M. E. Bahlke, S. Reineke, T. Van Voorhis, and M. A. Baldo, "External quantum efficiency above 100% in a singlet-exciton-fission-based organic photovoltaic cell," *Science* **340**, 334–337 (2013).
- <sup>42</sup>J. Lee, P. Jadhav, and M. A. Baldo, "High efficiency organic multilayer photodetectors based on singlet exciton fission," *Appl. Phys. Lett.* **95**, 033301 (2009).
- <sup>43</sup>M. D. Ediger, J. de Pablo, and L. Yu, "Anisotropic vapor-deposited glasses: Hybrid organic solids," *Acc. Chem. Res.* **52**, 407–414 (2019).
- <sup>44</sup>A. Gujral, L. Yu, and M. Ediger, "Anisotropic organic glasses," *Curr. Opin. Solid State Mater. Sci.* **22**, 49–57 (2018).
- <sup>45</sup>M. D. Ediger, "Perspective: Highly stable vapor-deposited glasses," *J. Chem. Phys.* **147**, 210901 (2017).
- <sup>46</sup>U. Heinemeyer, K. Broch, A. Hinderhofer, M. Kytka, R. Scholz, A. Gerlach, and F. Schreiber, "Real-time changes in the optical spectrum of organic semiconducting films and their thickness regimes during growth," *Phys. Rev. Lett.* **104**, 257401 (2010).
- <sup>47</sup>B. Krause, A. C. Dürr, K. Ritley, F. Schreiber, H. Dosch, and D. Smilgies, "Structure and growth morphology of an archetypal system for organic epitaxy: PTCDA on Ag(111)," *Phys. Rev. B* **66**, 235404 (2002).
- <sup>48</sup>J. O. Ossó, F. Schreiber, V. Kruppa, H. Dosch, M. Garriga, M. I. Alonso, and F. Cerdeira, "Controlled molecular alignment in phthalocyanine thin films on stepped sapphire surfaces," *Adv. Funct. Mater.* **12**, 455–460 (2002).
- <sup>49</sup>M. I. Alonso, M. Garriga, N. Karl, J. O. Ossó, and F. Schreiber, "Anisotropic optical properties of single crystalline PTCDA studied by spectroscopic ellipsometry," *Org. Electron.* **3**, 23–31 (2002).
- <sup>50</sup>I. Salzmann, G. Heimel, M. Oehzelt, S. Winkler, and N. Koch, "Molecular electrical doping of organic semiconductors: Fundamental mechanisms and emerging dopant design rules," *Acc. Chem. Res.* **49**, 370–378 (2016).
- <sup>51</sup>A. D. Scaccabarozzi, A. Basu, F. Aniés, J. Liu, O. Zapata-Arteaga, R. Warren, Y. Firdaus, M. I. Nugraha, Y. Lin, M. Campoy-Quiles, N. Koch, C. Müller, L. Tsetseris, M. Heeney, and T. D. Anthopoulos, "Doping approaches for organic semiconductors," *Chem. Rev.* **122**, 4420–4492 (2022).
- <sup>52</sup>M. L. Tietze, J. Benduhn, P. Pahner, B. Nell, M. Schwarze, H. Kleemann, M. Krammer, K. Zojer, K. Vandewal, and K. Leo, "Elementary steps in electrical doping of organic semiconductors," *Nat. Commun.* **9**, 1182 (2018).
- <sup>53</sup>L. Zhu, M. Zhang, J. Xu, C. Li, J. Yan, G. Zhou, W. Zhong, T. Hao, J. Song, X. Xue, Z. Zhou, R. Zeng, H. Zhu, C.-C. Chen, R. C. I. MacKenzie, Y. Zou, J. Nelson, Y. Zhang, Y. Sun, and F. Liu, "Single-junction organic solar cells with over 19% efficiency enabled by a refined double-fibril network morphology," *Nat. Mater.* **21**, 656–663 (2022).
- <sup>54</sup>A. A. Sifat, J. Jahng, and E. O. Potma, "Photo-induced force microscopy (PiFM) – Principles and implementations," *Chem. Soc. Rev.* **51**, 4208–4222 (2022).
- <sup>55</sup>A. Amorim da Costa, A. Amado, M. Becucci, and C. Kryschi, "Order-disorder phase transition in p-terphenyl and p-terphenyl: Tetracene doped crystals as studied by Raman spectroscopy," *J. Mol. Struct.* **416**, 69–73 (1997).
- <sup>56</sup>E. Fratzczak, P. Uznanski, and M. Moneta, "Characterization of molecular organization in pentacene thin films on SiO<sub>2</sub> surface using infrared spectroscopy, spectroscopic ellipsometry, and atomic force microscopy," *Chem. Phys.* **456**, 49–56 (2015).
- <sup>57</sup>K. Hubenko, A. Kusber, M. Naumann, B. Büchner, and M. Knupfer, "Evolution of the pentacene exciton band width in pentacene-tetracene blends," *J. Chem. Phys.* **160**, 144708 (2024).
- <sup>58</sup>K. Broch, J. Dieterle, F. Branchi, N. J. Hestand, Y. Olivier, H. Tamura, C. Cruz, V. M. Nichols, A. Hinderhofer, D. Beljonne, F. C. Spano, G. Cerullo, C. J. Bardeen, and F. Schreiber, "Robust singlet fission in pentacene thin films with tuned charge transfer interactions," *Nat. Commun.* **9**, 954 (2018).
- <sup>59</sup>K. Broch, A. Aufderheide, L. Raimondo, A. Sassella, A. Gerlach, and F. Schreiber, "Optical properties of blends: Influence of mixing-induced disorder in pentacene: Diindenoperylene versus perfluoropentacene: Diindenoperylene," *J. Phys. Chem. C* **117**, 13952–13960 (2013).
- <sup>60</sup>C. P. Theurer, M. Richter, D. Rana, G. Duva, D. Lepple, A. Hinderhofer, F. Schreiber, P. Tegeder, and K. Broch, "Coexistence of ion pairs and charge-transfer complexes and their impact on pentacene singlet fission," *J. Phys. Chem. C* **125**, 23952–23959 (2021).
- <sup>61</sup>K. Broch, U. Heinemeyer, A. Hinderhofer, F. Anger, R. Scholz, A. Gerlach, and F. Schreiber, "Optical evidence for intermolecular coupling in mixed films of pentacene and perfluoropentacene," *Phys. Rev. B* **83**, 245307 (2011).
- <sup>62</sup>A. Hinderhofer, C. Frank, T. Hosokai, A. Resta, A. Gerlach, and F. Schreiber, "Structure and morphology of coevaporated pentacene-perfluoropentacene thin films," *J. Chem. Phys.* **134**(10), 104702 (2011).
- <sup>63</sup>J. Dieterle, K. Broch, A. Hinderhofer, H. Frank, J. Novák, A. Gerlach, T. Breuer, R. Banerjee, G. Witte, and F. Schreiber, "Structural properties of picene-perfluoropentacene and picene-pentacene blends: Superlattice formation versus limited intermixing," *J. Phys. Chem. C* **119**(47), 26339–26347 (2015).
- <sup>64</sup>J. Dieterle, K. Broch, H. Frank, G. Duva, T. Storzer, A. Hinderhofer, J. Novák, A. Gerlach, and F. Schreiber, "Delayed phase separation in growth of organic semiconductor blends with limited intermixing," *Phys. Status Solidi RRL* **11**, 1600428 (2017).
- <sup>65</sup>C. Zeiser, L. Moretti, D. Lepple, G. Cerullo, M. Maiuri, and K. Broch, "Singlet heterofission in tetracene-pentacene thin-film blends," *Angew. Chem.* **132**, 20141–20148 (2020).
- <sup>66</sup>A. Aufderheide, K. Broch, J. Novák, A. Hinderhofer, R. Nervo, A. Gerlach, R. Banerjee, and F. Schreiber, "Mixing-induced anisotropic correlations in molecular crystalline systems," *Phys. Rev. Lett.* **109**, 156102 (2012).
- <sup>67</sup>Y. Iwasawa and Y. Furukawa, "Raman study on a bulk-heterojunction film of pentacene and C<sub>60</sub>," *Chem. Phys. Lett.* **636**, 58–61 (2015).

- <sup>68</sup>Y. Zheng, S. K. Pregler, J. D. Myers, J. Ouyang, S. B. Sinnott, and J. Xue, "Computational and experimental studies of phase separation in pentacene: C<sub>60</sub> mixtures," *J. Vac. Sci. Technol., B* **27**(1), 169–179 (2009).
- <sup>69</sup>A. Hinderhofer and F. Schreiber, "Organic–organic heterostructures: Concepts and applications," *ChemPhysChem* **13**, 628–643 (2012).
- <sup>70</sup>D. Lubert-Perquel, E. Salvadori, M. Dyson, P. N. Stavrinou, R. Montis, H. Nagashima, Y. Kobori, S. Heutz, and C. W. M. Kay, "Identifying triplet pathways in dilute pentacene films," *Nat. Commun.* **9**, 4222 (2018).
- <sup>71</sup>A. I. Kitaigorodsky, *Mixed Crystals* (Springer Berlin Heidelberg, 1984).
- <sup>72</sup>K. A. Dill, S. Bromberg, and D. Stigter, *Molecular Driving Forces: Statistical Thermodynamics in Chemistry and Biology* (Garland Science, New York, 2011).
- <sup>73</sup>A. I. Kitaigorodsky, *Molecular Crystals and Molecules* (Academic Press, New York, 1973).
- <sup>74</sup>A. Hinderhofer, T. Hosokai, C. Frank, J. Novák, A. Gerlach, and F. Schreiber, "Templating effect for organic heterostructure film growth: Perfluoropentacene on diindenoperylene," *J. Phys. Chem. C* **115**, 16155–16160 (2011).
- <sup>75</sup>M. K. Corpinot and D.-K. Bučar, "A practical guide to the design of molecular crystals," *Cryst. Growth Des.* **19**, 1426–1453 (2019).
- <sup>76</sup>A. Opitz, J. Wagner, W. Brütting, I. Salzmann, N. Koch, J. Manara, J. Pflaum, A. Hinderhofer, and F. Schreiber, "Charge separation at molecular donor–acceptor interfaces: Correlation between morphology and solar cell performance," *IEEE J. Sel. Top. Quantum Electron.* **16**, 1707–1717 (2010).
- <sup>77</sup>C. R. Taylor and G. M. Day, "Evaluating the energetic driving force for cocrystal formation," *Cryst. Growth Des.* **18**, 892–904 (2018).
- <sup>78</sup>S. W. Watt, C. Dai, A. J. Scott, J. M. Burke, R. L. Thomas, J. C. Collings, C. Viney, W. Clegg, and T. B. Marder, "Structure and phase behavior of a 2:1 complex between arene- and fluoroarene-based conjugated rigid rods," *Angew. Chem.* **116**, 3123–3125 (2004).
- <sup>79</sup>S. Price, "Molecular crystals," in *Computer Modeling in Inorganic Crystallography* (Elsevier, 1997), pp. 269–293.
- <sup>80</sup>J. Nyman and G. M. Day, "Static and lattice vibrational energy differences between polymorphs," *CrystEngComm* **17**, 5154–5165 (2015).
- <sup>81</sup>S. L. Price, "Control and prediction of the organic solid state: A challenge to theory and experiment," *Proc. R. Soc. A* **474**, 20180351 (2018).
- <sup>82</sup>M. Klues and G. Witte, "Crystalline packing in pentacene-like organic semiconductors," *CrystEngComm* **20**, 63–74 (2018).
- <sup>83</sup>R. K. Nahm and J. R. Engstrom, "Who's on first? Tracking in real time the growth of multiple crystalline phases of an organic semiconductor: Tetracene on SiO<sub>2</sub>," *J. Chem. Phys.* **146**, 052815 (2017).
- <sup>84</sup>Y. Su, Z.-F. Yao, B. Wu, Y.-D. Zhao, J.-Y. Han, J.-H. Sun, M.-P. Zhuo, J.-Z. Fan, Z.-S. Wang, J. Pei, L.-S. Liao, and X.-D. Wang, "Organic polymorph-based alloys for continuous regulation of emission colors," *Matter* **5**, 1520–1531 (2022).
- <sup>85</sup>E. Venuti, R. G. Della Valle, A. Brillante, M. Masino, and A. Girlando, "Probing pentacene polymorphs by lattice dynamics calculations," *J. Am. Chem. Soc.* **124**, 2128–2129 (2002).
- <sup>86</sup>R. G. Della Valle, E. Venuti, A. Brillante, and A. Girlando, "Inherent structures of crystalline pentacene," *J. Chem. Phys.* **118**, 807–815 (2003).
- <sup>87</sup>J. Bernstein, *Polymorphism in Molecular Crystals*, 2nd ed. (Oxford University Press, 2020).
- <sup>88</sup>P. Beyer, D. Pham, C. Peter, N. Koch, E. Meister, W. Brütting, L. Grubert, S. Hecht, D. Nabok, C. Cocchi, C. Draxl, and A. Opitz, "State-of-matter-dependent charge-transfer interactions between planar molecules for doping applications," *Chem. Mater.* **31**, 1237–1249 (2019).
- <sup>89</sup>A. Opitz, C. Peter, B. Wegner, H. R. Matte, A. Röttger, T. Florian, X. Xu, P. Beyer, L. Grubert, S. Hecht, V. Belova, A. Hinderhofer, F. Schreiber, C. Kasper, J. Pflaum, Y. Zhang, S. Barlow, S. R. Marder, and N. Koch, "Ordered donor–acceptor complex formation and electron transfer in co-deposited films of structurally dissimilar molecules," *J. Phys. Chem. C* **124**, 11023–11031 (2020).
- <sup>90</sup>I. Salzmann, R. Opitz, S. Rogaschewski, J. P. Rabe, N. Koch, and B. Nickel, "Phase separation in vacuum codeposited pentacene/6,13-pentacenequinone thin films," *Phys. Rev. B* **75**, 174108 (2007).
- <sup>91</sup>G. M. Akselrod, P. B. Deotare, N. J. Thompson, J. Lee, W. A. Tisdale, M. A. Baldo, V. M. Menon, and V. Bulović, "Visualization of exciton transport in ordered and disordered molecular solids," *Nat. Commun.* **5**, 3646 (2014).
- <sup>92</sup>L. Craciunescu, S. Wirsing, S. Hammer, K. Broch, A. Dreuw, F. Fantuzzi, V. Sivanesan, P. Tegeder, and B. Engels, "Accurate polarization-resolved absorption spectra of organic semiconductor thin films using first-principles quantum-chemical methods: Pentacene as a case study," *J. Phys. Chem. Lett.* **13**, 3726–3731 (2022).
- <sup>93</sup>L. Craciunescu, M. Asbach, S. Wirsing, S. Hammer, F. Unger, K. Broch, F. Schreiber, G. Witte, A. Dreuw, P. Tegeder, F. Fantuzzi, and B. Engels, "Cluster-based approach utilizing optimally tuned TD-DFT to calculate absorption spectra of organic semiconductor thin films," *J. Chem. Theory Comput.* **19**, 9369 (2023).
- <sup>94</sup>F. Schreiber, "Organic molecular beam deposition: Growth studies beyond the first monolayer," *Phys. Status Solidi A* **201**, 1037–1054 (2004).
- <sup>95</sup>S. R. Forrest, "Ultrathin organic films grown by organic molecular beam deposition and related techniques," *Chem. Rev.* **97**, 1793–1896 (1997).
- <sup>96</sup>R. Banerjee, J. Novák, C. Frank, C. Lorch, A. Hinderhofer, A. Gerlach, and F. Schreiber, "Evidence for kinetically limited thickness dependent phase separation in organic thin film blends," *Phys. Rev. Lett.* **110**, 185506 (2013).
- <sup>97</sup>G. R. Desiraju, "Crystal engineering: From molecule to crystal," *J. Am. Chem. Soc.* **135**, 9952–9967 (2013).
- <sup>98</sup>C. Lorch, H. Frank, R. Banerjee, A. Hinderhofer, A. Gerlach, G. Li Destri, and F. Schreiber, "Controlling length-scales of the phase separation to optimize organic semiconductor blends," *Appl. Phys. Lett.* **107**, 201603 (2015).
- <sup>99</sup>R. Banerjee, A. Hinderhofer, M. Weinmann, B. Reisz, C. Lorch, A. Gerlach, M. Oettel, and F. Schreiber, "Interrupted growth to manipulate phase separation in DIP: C60 organic semiconductor blends," *J. Phys. Chem. C* **122**, 1839–1845 (2018).
- <sup>100</sup>J. Zhang, I. Salzmann, S. Rogaschewski, J. P. Rabe, N. Koch, F. Zhang, and Z. Xu, "Arrays of crystalline C<sub>60</sub> and pentacene nanocolumns," *Appl. Phys. Lett.* **90**, 193117 (2007).
- <sup>101</sup>L. Pithan, C. Cocchi, H. Zschiesche, C. Weber, A. Zykov, S. Bommel, S. J. Leake, P. Schäfer, C. Draxl, and S. Kowarik, "Light controls polymorphism in thin films of sexithiophene," *Cryst. Growth Des.* **15**, 1319–1324 (2015).
- <sup>102</sup>D. Holmes, S. Kumaraswamy, A. J. Matzger, and K. P. C. Vollhardt, "On the nature of nonplanarity in the [n]phenylenes," *Chem. Eur. J.* **5**, 3399–3412 (1999).
- <sup>103</sup>C. C. Mattheus, A. B. Dros, J. Baas, G. T. Oostergetel, A. Meetsma, J. L. de Boer, and T. T. Palstra, "Identification of polymorphs of pentacene," *Synth. Met.* **138**, 475–481 (2003).
- <sup>104</sup>S. Schiefer, M. Huth, A. Dobrinevski, and B. Nickel, "Determination of the crystal structure of substrate-induced pentacene polymorphs in fiber structured thin films," *J. Am. Chem. Soc.* **129**, 10316–10317 (2007).
- <sup>105</sup>R. G. Della Valle, A. Brillante, L. Farina, E. Venuti, M. Masino, and A. Girlando, "Organic semiconductors: Polymorphism, phonon dynamics and carrier-phonon coupling in pentacene," *Mol. Cryst. Liq. Cryst.* **416**, 145–154 (2004).
- <sup>106</sup>R. B. Campbell, J. M. Robertson, and J. Trotter, "The crystal structure of hexacene, and a revision of the crystallographic data for tetracene and pentacene," *Acta Cryst.* **15**, 289–290 (1962).
- <sup>107</sup>A. C. Mayer, A. Kazimirov, and G. G. Malliaras, "Dynamics of bimodal growth in pentacene thin films," *Phys. Rev. Lett.* **97**, 105503 (2006).
- <sup>108</sup>I. Meyenburg, T. Breuer, A. Karthäuser, S. Chatterjee, G. Witte, and W. Heimbrodt, "Temperature-resolved optical spectroscopy of pentacene polymorphs: Variation of herringbone angles in single-crystals and interface-controlled thin films," *Phys. Chem. Chem. Phys.* **18**, 3825–3831 (2016).
- <sup>109</sup>D. Nabok, P. Puschnig, C. Ambrosch-Draxl, O. Werzer, R. Resel, and D.-M. Smilgies, "Crystal and electronic structures of pentacene thin films from grazing-incidence x-ray diffraction and first-principles calculations," *Phys. Rev. B* **76**, 235322 (2007).
- <sup>110</sup>K. Broch, C. Bürker, J. Dieterle, S. Krause, A. Gerlach, and F. Schreiber, "Impact of molecular tilt angle on the absorption spectra of pentacene: Perfluoropentacene blends," *Phys. Status Solidi RRL* **7**, 1084–1088 (2013).
- <sup>111</sup>S. E. Fritz, S. M. Martin, C. D. Frisbie, M. D. Ward, and M. F. Toney, "Structural characterization of a pentacene monolayer on an amorphous SiO<sub>2</sub> substrate with grazing incidence X-ray diffraction," *J. Am. Chem. Soc.* **126**, 4084–4085 (2004).
- <sup>112</sup>D. Käfer, C. Wöll, and G. Witte, "Thermally activated dewetting of organic thin films: The case of pentacene on SiO<sub>2</sub> and gold," *Appl. Phys. A* **95**, 273–284 (2009).

- <sup>113</sup>G. Yoshikawa, T. Miyadera, R. Onoki, K. Ueno, I. Nakai, S. Entani, S. Ikeda, D. Guo, M. Kiguchi, H. Kondoh, T. Ohta, and K. Saiki, "In-situ measurement of molecular orientation of the pentacene ultrathin films grown on SiO<sub>2</sub> substrates," *Surf. Sci.* **600**, 2518–2522 (2006).
- <sup>114</sup>G. Witte and C. Wöll, "Growth of aromatic molecules on solid substrates for applications in organic electronics," *J. Mater. Res.* **19**, 1889–1916 (2004).
- <sup>115</sup>I. Bouchoms, W. Schoonveld, J. Vrijmoeth, and T. Klapwijk, "Morphology identification of the thin film phases of vacuum evaporated pentacene on SiO<sub>2</sub> substrates," *Synth. Met.* **104**, 175–178 (1999).
- <sup>116</sup>H. Yoshida and N. Sato, "Grazing-incidence x-ray diffraction study of pentacene thin films with the bulk phase structure," *Appl. Phys. Lett.* **89**, 101919 (2006).
- <sup>117</sup>L. Pithan, D. Nabok, C. Cocchi, P. Beyer, G. Duva, J. Simbrunner, J. Rawle, C. Nicklin, P. Schäfer, C. Draxl, F. Schreiber, and S. Kowarik, "Molecular structure of the substrate-induced thin-film phase of tetracene," *J. Chem. Phys.* **149**, 144701 (2018).
- <sup>118</sup>N. Shioya, K. Eda, T. Shimoaka, and T. Hasegawa, "Hidden thin-film phase of dinaphthothienothiophene revealed by high-resolution X-ray diffraction," *Appl. Phys. Express* **13**, 095505 (2020).
- <sup>119</sup>A. Hinderhofer, T. Hosokai, K. Yonezawa, A. Gerlach, K. Kato, K. Broch, C. Frank, J. Novák, S. Kera, N. Ueno, and F. Schreiber, "Post-growth surface smoothing of thin films of diindenoperylene," *Appl. Phys. Lett.* **101**, 033307 (2012).
- <sup>120</sup>A. C. Dürr, F. Schreiber, M. Münch, N. Karl, B. Krause, V. Kruppa, and H. Dosch, "High structural order in thin films of the organic semiconductor diindenoperylene," *Appl. Phys. Lett.* **81**, 2276–2278 (2002).
- <sup>121</sup>T. Siegrist, C. Kloc, J. H. Schön, B. Batlogg, R. C. Haddon, S. Berg, and G. A. Thomas, "Enhanced physical properties in a pentacene polymorph," *Angew. Chem., Int. Ed.* **40**, 1732–1736 (2001).
- <sup>122</sup>A. S. Davydov, "The theory of molecular excitons," *Sov. Phys. Usp.* **7**, 145–178 (1964).
- <sup>123</sup>M. Kasha, H. R. Rawls, and M. Ashraf El-Bayoumi, "The exciton model in molecular spectroscopy," *Pure Appl. Chem.* **11**, 371–392 (1965).
- <sup>124</sup>F. C. Spano, "The spectral signatures of Frenkel polarons in H- and J-aggregates," *Acc. Chem. Res.* **43**, 429–439 (2010).
- <sup>125</sup>M. L. Tiago, J. E. Northrup, and S. G. Louie, "Ab initio calculation of the electronic and optical properties of solid pentacene," *Phys. Rev. B* **67**, 115212 (2003).
- <sup>126</sup>P. Petelenz, M. Snamina, and G. Mazur, "Charge-transfer states in pentacene: Dimer versus crystal," *J. Phys. Chem. C* **119**, 14338–14342 (2015).
- <sup>127</sup>N. J. Hestand, H. Yamagata, B. Xu, D. Sun, Y. Zhong, A. R. Harutyunyan, G. Chen, H.-L. Dai, Y. Rao, and F. C. Spano, "Polarized absorption in crystalline pentacene: Theory vs experiment," *J. Phys. Chem. C* **119**, 22137–22147 (2015).
- <sup>128</sup>D. Beljonne, H. Yamagata, J. L. Brédas, F. C. Spano, and Y. Olivier, "Charge-transfer excitations steer the Davydov splitting and mediate singlet exciton fission in pentacene," *Phys. Rev. Lett.* **110**, 226402 (2013).
- <sup>129</sup>H. Yamagata, J. Norton, E. Hontz, Y. Olivier, D. Beljonne, J. L. Brédas, R. J. Silbey, and F. C. Spano, "The nature of singlet excitons in oligoacene molecular crystals," *J. Chem. Phys.* **134**, 204703 (2011).
- <sup>130</sup>B. Alam, A. F. Morrison, and J. M. Herbert, "Charge separation and charge transfer in the low-lying excited states of pentacene," *J. Phys. Chem. C* **124**, 24653–24666 (2020).
- <sup>131</sup>F. Plasser and H. Lischka, "Analysis of excitonic and charge transfer interactions from quantum chemical calculations," *J. Chem. Theory Comput.* **8**, 2777–2789 (2012).
- <sup>132</sup>F. Plasser, "TheoDOR: A toolbox for a detailed and automated analysis of electronic excited state computations," *J. Chem. Phys.* **152**, 084108 (2020).
- <sup>133</sup>L. Sebastian, G. Weiser, and H. Bässler, "Charge transfer transitions in solid tetracene and pentacene studied by electroabsorption," *Chem. Phys.* **61**, 125–135 (1981).
- <sup>134</sup>S. Haas, H. Matsui, and T. Hasegawa, "Field-modulation spectroscopy of pentacene thin films using field-effect devices: Reconsideration of the excitonic structure," *Phys. Rev. B* **82**, 161301 (2010).
- <sup>135</sup>M. Dressel, B. Gompf, D. Faltermeier, A. K. Tripathi, J. Pflaum, and M. Schubert, "Kramers-Kronig-consistent optical functions of anisotropic crystals: Generalized spectroscopic ellipsometry on pentacene," *Opt. Express* **16**, 19770–19778 (2008).
- <sup>136</sup>P. Cudazzo, M. Gatti, and A. Rubio, "Excitons in molecular crystals from first-principles many-body perturbation theory: Picene versus pentacene," *Phys. Rev. B* **86**, 195307 (2012).
- <sup>137</sup>D. Faltermeier, B. Gompf, M. Dressel, A. K. Tripathi, and J. Pflaum, "Optical properties of pentacene thin films and single crystals," *Phys. Rev. B* **74**, 125416 (2006).
- <sup>138</sup>G. Duva, A. Mann, L. Pithan, P. Beyer, J. Hagenlocher, A. Gerlach, A. Hinderhofer, and F. Schreiber, "Template-free orientation selection of rod-like molecular semiconductors in polycrystalline films," *J. Phys. Chem. Lett.* **10**, 1031–1036 (2019).
- <sup>139</sup>N. Shioya, R. Murdey, K. Nakao, H. Yoshida, T. Koganezawa, K. Eda, T. Shimoaka, and T. Hasegawa, "Alternative face-on thin film structure of pentacene," *Sci. Rep.* **9**, 579 (2019).
- <sup>140</sup>K. Kim, E. J. G. Santos, T. H. Lee, Y. Nishi, and Z. Bao, "Epitaxially grown strained pentacene thin film on graphene membrane," *Small* **11**, 2037–2043 (2015).
- <sup>141</sup>M. Shibuta and A. Nakajima, "Imaging of ultrafast photoexcited electron dynamics in pentacene nanocrystals on a graphite substrate," *Nanoscale* **16**, 12397–12405 (2024).
- <sup>142</sup>C. Cocchi, M. Guerrini, J. Krumland, N. Trung Nguyen, and A. M. Valencia, "Modeling the electronic structure of organic materials: A solid-state physicist's perspective," *J. Phys. Mater.* **6**, 012001 (2023).
- <sup>143</sup>T. Zeng, R. Hoffmann, and N. Ananth, "The low-lying electronic states of pentacene and their roles in singlet fission," *J. Am. Chem. Soc.* **136**, 5755–5764 (2014).
- <sup>144</sup>P. M. Zimmerman, Z. Zhang, and C. B. Musgrave, "Singlet fission in pentacene through multi-exciton quantum states," *Nat. Chem.* **2**, 648–652 (2010).
- <sup>145</sup>S. Refaely-Abramson, F. H. da Jornada, S. G. Louie, and J. B. Neaton, "Origins of singlet fission in solid pentacene from an ab initio Green's function approach," *Phys. Rev. Lett.* **119**, 267401 (2017).
- <sup>146</sup>Y. Yang, E. R. Davidson, and W. Yang, "Nature of ground and electronic excited states of higher acenes," *Proc. Natl. Acad. Sci. U. S. A.* **113**, E5098–E5107 (2016).
- <sup>147</sup>F.-J. Meyer zur Heringdorf, M. C. Reuter, and R. M. Tromp, "Growth dynamics of pentacene thin films," *Nature* **412**, 517–520 (2001).
- <sup>148</sup>R. Ruiz, D. Choudhary, B. Nickel, T. Toccoli, K.-C. Chang, A. C. Mayer, P. Clancy, J. M. Blakely, R. L. Headrick, S. Iannotta, and G. G. Malliaras, "Pentacene thin film growth," *Chem. Mater.* **16**, 4497–4508 (2004).
- <sup>149</sup>D. Guo, S. Ikeda, and K. Saiki, "Modified bimodal growth mechanism of pentacene thin films at elevated substrate temperatures," *J. Phys.: Condens. Matter* **22**, 262001 (2010).
- <sup>150</sup>A. P. Rice, F. S. Tham, and E. L. Chronister, "A temperature dependent x-ray study of the order-disorder enantiotropic phase transition of p-terphenyl," *J. Chem. Crystallogr.* **43**, 14–25 (2013).
- <sup>151</sup>M. Watanabe, Y. J. Chang, S.-W. Liu, T.-H. Chao, K. Goto, M. M. Islam, C.-H. Yuan, Y.-T. Tao, T. Shinmyozu, and T. J. Chow, "The synthesis, crystal structure and charge-transport properties of hexacene," *Nat. Chem.* **4**, 574–578 (2012).
- <sup>152</sup>M. Mamada, H. Katagiri, M. Mizukami, K. Honda, T. Minamiki, R. Teraoka, T. Uemura, and S. Tokito, "syn-/anti-anthradithiophene derivative isomer effects on semiconducting properties," *ACS Appl. Mater. Interfaces* **5**, 9670–9677 (2013).
- <sup>153</sup>T. Yamamoto and K. Takimiya, "Facile synthesis of highly  $\pi$ -extended heteroarenes, dinaphtho[2,3-b:2',3'-f]chalcogenopheno[3,2-b]chalcogenophenes, and their application to field-effect transistors," *J. Am. Chem. Soc.* **129**, 2224–2225 (2007).
- <sup>154</sup>A. De, R. Ghosh, S. Roychowdhury, and P. Roychowdhury, "Structural analysis of picene, C<sub>22</sub>H<sub>14</sub>," *Acta Crystallogr., Sect. C* **41**, 907–909 (1985).
- <sup>155</sup>D. M. Burns and J. Iball, "Refinement of the structure of chrysene," *Proc. R. Soc. London, Ser. A* **257**, 491–514 (1960).
- <sup>156</sup>N. Hofeditz, J. Hausch, K. Broch, W. Heimbrodt, F. Schreiber, and M. Gerhard, "Efficient energy transfer and singlet fission in co-deposited thin films of pentacene and anthradithiophene," *Adv. Mater. Interfaces* **11**, 2300922 (2024).
- <sup>157</sup>A. Musa, M. Saeed, A. Shaari, R. Sahnoun, and M. Lawal, "Effects of delocalised  $\pi$ -electrons around the linear acenes ring (n = 1 to 7): An electronic

- properties through DFT and quantum chemical descriptors,” *Mol. Phys.* **113**, 1347–1358 (2015).
- <sup>158</sup>W. N. Han, K. Yonezawa, R. Makino, K. Kato, A. Hinderhofer, R. Murdey, R. Shiraiishi, H. Yoshida, N. Sato, N. Ueno, and S. Kera, “Quantitatively identical orientation-dependent ionization energy and electron affinity of diindenoperylene,” *Appl. Phys. Lett.* **103**, 253301 (2013).
- <sup>159</sup>A. Hinderhofer, A. Gerlach, K. Broch, T. Hosokai, K. Yonezawa, K. Kato, S. Kera, N. Ueno, and F. Schreiber, “Geometric and electronic structure of templated C<sub>60</sub> on diindenoperylene thin films,” *J. Phys. Chem. C* **117**, 1053–1058 (2013).
- <sup>160</sup>D.-M. Smilgies, “Scherrer grain-size analysis adapted to grazing-incidence scattering with area detectors,” *J. Appl. Crystallogr.* **42**, 1030–1034 (2009).
- <sup>161</sup>A. Opitz, B. Ecker, J. Wagner, A. Hinderhofer, F. Schreiber, J. Manara, J. Pflaum, and W. Brütting, “Mixed crystalline films of co-evaporated hydrogen- and fluorine-terminated phthalocyanines and their application in photovoltaic devices,” *Org. Electron.* **10**, 1259–1267 (2009).
- <sup>162</sup>L. Vegard, “Die Konstitution der Mischkristalle und die Raumfüllung der Atome,” *Z. Phys.* **5**, 17–26 (1921).
- <sup>163</sup>S. Kowarik, A. Gerlach, S. Sellner, F. Schreiber, J. Pflaum, L. Cavalcanti, and O. Kononov, “Anomalous roughness evolution of rubrene thin films observed in real time during growth,” *Phys. Chem. Chem. Phys.* **8**, 1834–1836 (2006).
- <sup>164</sup>N. I. Wakayama, S. Matsuzaki, and M. Mizuno, “UV absorption study of the phase transition in *p*-terphenyl crystal,” *Chem. Phys. Lett.* **75**, 587–589 (1980).
- <sup>165</sup>H. Rietveld, E. Maslen, and C. Clews, “An X-ray and neutron diffraction refinement of the structure of *p*-terphenyl,” *Acta Crystallogr., Sect. B* **26**, 693–706 (1970).
- <sup>166</sup>R. M. Myasnikova, “Lattice distortions in organic solid solutions,” *Mol. Cryst. Liq. Cryst.* **90**, 195–204 (1983).
- <sup>167</sup>M. Sawatzki-Park, S.-J. Wang, H. Kleemann, and K. Leo, “Highly ordered small molecule organic semiconductor thin-films enabling complex, high-performance multi-junction devices,” *Chem. Rev.* **123**, 8232–8250 (2023).
- <sup>168</sup>P. Friederich, V. Meded, A. Poschlad, T. Neumann, V. Rodin, V. Stehr, F. Symalla, D. Danilov, G. Lüdemann, R. F. Fink, I. Kondov, F. von Wrochem, and W. Wenzel, “Molecular origin of the charge carrier mobility in small molecule organic semiconductors,” *Adv. Funct. Mater.* **26**, 5757–5763 (2016).
- <sup>169</sup>S. Sharifzadeh, P. Darancet, L. Kronik, and J. B. Neaton, “Low-energy charge-transfer excitons in organic solids from first-principles: The case of pentacene,” *J. Phys. Chem. Lett.* **4**, 2197–2201 (2013).
- <sup>170</sup>F. Roth, R. Schuster, A. König, M. Knupfer, and H. Berger, “Momentum dependence of the excitons in pentacene,” *J. Chem. Phys.* **136**, 204708 (2012).
- <sup>171</sup>P. Hervé and L. Vandamme, “General relation between refractive index and energy gap in semiconductors,” *Infrared Phys. Technol.* **35**, 609–615 (1994).
- <sup>172</sup>T. Tian, D. Scullion, D. Hughes, L. H. Li, C.-J. Shih, J. Coleman, M. Chhowalla, and E. J. G. Santos, “Electronic polarizability as the fundamental variable in the dielectric properties of two-dimensional materials,” *Nano Lett.* **20**, 841–851 (2020).
- <sup>173</sup>D. Lubert-Perquel, D. K. Kim, P. Robaschik, C. W. M. Kay, and S. Heutz, “Growth, morphology and structure of mixed pentacene films,” *J. Mater. Chem. C* **7**, 289–296 (2019).
- <sup>174</sup>X. Huang, X. Liu, K. Ding, and S. R. Forrest, “Is there such a thing as a molecular organic alloy?” *Mater. Horiz.* **7**, 244–251 (2020).
- <sup>175</sup>I. Salzmänn, S. Duhm, R. Opitz, R. L. Johnson, J. P. Rabe, and N. Koch, “Structural and electronic properties of pentacene-fullerene heterojunctions,” *J. Appl. Phys.* **104**, 114518 (2008).
- <sup>176</sup>A. Rao, M. W. B. Wilson, J. M. Hodgkiss, S. Albert-Seifried, H. Bässler, and R. H. Friend, “Exciton fission and charge generation via triplet excitons in pentacene/C<sub>60</sub> bilayers,” *J. Am. Chem. Soc.* **132**, 12698–12703 (2010).
- <sup>177</sup>S. Yoo, B. Domercq, and B. Kippelen, “Efficient thin-film organic solar cells based on pentacene/C<sub>60</sub> heterojunctions,” *Appl. Phys. Lett.* **85**, 5427–5429 (2004).
- <sup>178</sup>M. Tabachnyk, B. Ehrler, S. Bayliss, R. H. Friend, and N. C. Greenham, “Triplet diffusion in singlet exciton fission sensitized pentacene solar cells,” *Appl. Phys. Lett.* **103**, 153302 (2013).
- <sup>179</sup>T. Breuer, T. Geiger, H. F. Bettinger, and G. Witte, “Diels-Alder adduct formation at solid interfaces between fullerenes and acenes,” *J. Phys.: Condens. Matter* **31**, 034003 (2019).
- <sup>180</sup>C. Cocchi, T. Breuer, G. Witte, and C. Draxl, “Polarized absorbance and Davydov splitting in bulk and thin-film pentacene polymorphs,” *Phys. Chem. Chem. Phys.* **20**, 29724–29736 (2018).
- <sup>181</sup>S. Varghese and S. Das, “Role of molecular packing in determining solid-state optical properties of  $\pi$ -conjugated materials,” *J. Phys. Chem. Lett.* **2**, 863–873 (2011).
- <sup>182</sup>C. Grieco, G. S. Doucette, R. D. Pensack, M. M. Payne, A. Rimshaw, G. D. Scholes, J. E. Anthony, and J. B. Asbury, “Dynamic exchange during triplet transport in nanocrystalline TIPS-pentacene films,” *J. Am. Chem. Soc.* **138**, 16069–16080 (2016).
- <sup>183</sup>J.-O. Vogel, I. Salzmänn, S. Duhm, M. Oehzelt, J. P. Rabe, and N. Koch, “Phase-separation and mixing in thin films of co-deposited rod-like conjugated molecules,” *J. Mater. Chem.* **20**, 4055–4066 (2010).
- <sup>184</sup>I. Salzmänn, S. Duhm, G. Heimel, J. P. Rabe, N. Koch, M. Oehzelt, Y. Sakamoto, and T. Suzuki, “Structural order in perfluoropentacene thin films and heterostructures with pentacene,” *Langmuir* **24**, 7294–7298 (2008).
- <sup>185</sup>F. Anger, J. O. Ossó, U. Heinemeyer, K. Broch, R. Scholz, A. Gerlach, and F. Schreiber, “Photoluminescence spectroscopy of pure pentacene, perfluoropentacene, and mixed thin films,” *J. Chem. Phys.* **136**, 054701 (2012).
- <sup>186</sup>T. Breuer and G. Witte, “Thermally activated intermixture in pentacene-perfluoropentacene heterostructures,” *J. Chem. Phys.* **138**, 114901 (2013).
- <sup>187</sup>K. Broch, M. Gerhard, M. Halbach, S. Lippert, V. Belova, M. Koch, and F. Schreiber, “Time-resolved photoluminescence spectroscopy of charge transfer states in blends of pentacene and perfluoropentacene,” *Phys. Status Solidi RRL* **11**, 1700064 (2017).
- <sup>188</sup>A. Rinn, T. Breuer, J. Wiegand, M. Beck, J. Hübner, R. C. Döring, M. Oestreich, W. Heimbrot, G. Witte, and S. Chatterjee, “Interfacial molecular packing determines exciton dynamics in molecular heterostructures: The case of pentacene-perfluoropentacene,” *ACS Appl. Mater. Interfaces* **9**, 42020–42028 (2017).
- <sup>189</sup>V. O. Kim, K. Broch, V. Belova, Y. S. Chen, A. Gerlach, F. Schreiber, H. Tamura, R. G. Della Valle, G. D’Avino, I. Salzmänn, D. Beljonne, A. Rao, and R. Friend, “Singlet exciton fission via an intermolecular charge transfer state in coevaporated pentacene-perfluoropentacene thin films,” *J. Chem. Phys.* **151**, 164706 (2019).
- <sup>190</sup>D. Günder, A. M. Valencia, M. Guerrini, T. Breuer, C. Cocchi, and G. Witte, “Polarization resolved optical excitation of charge-transfer excitons in PEN:PF6 cocrystalline films: Limits of nonperiodic modeling,” *J. Phys. Chem. Lett.* **12**, 9899–9905 (2021).
- <sup>191</sup>J. H. Williams, “The molecular electric quadrupole moment and solid-state architecture,” *Acc. Chem. Res.* **26**, 593–598 (1993).
- <sup>192</sup>A. Hinderhofer, U. Heinemeyer, A. Gerlach, S. Kowarik, R. M. J. Jacobs, Y. Sakamoto, T. Suzuki, and F. Schreiber, “Optical properties of pentacene and perfluoropentacene thin films,” *J. Chem. Phys.* **127**, 194705 (2007).
- <sup>193</sup>S. Hammer, C. Zeiser, M. Deutsch, B. Engels, K. Broch, and J. Pflaum, “Spatial anisotropy of charge transfer at perfluoropentacene-pentacene (001) single-crystal interfaces and its relevance for thin film devices,” *ACS Appl. Mater. Interfaces* **12**, 53547–53556 (2020).
- <sup>194</sup>I. Salzmänn, G. Heimel, S. Duhm, M. Oehzelt, P. Pingel, B. M. George, A. Schnegg, K. Lips, R.-P. Blum, A. Vollmer, and N. Koch, “Intermolecular hybridization governs molecular electrical doping,” *Phys. Rev. Lett.* **108**, 035502 (2012).
- <sup>195</sup>S. D. Ha and A. Kahn, “Isolated molecular dopants in pentacene observed by scanning tunneling microscopy,” *Phys. Rev. B* **80**, 195410 (2009).
- <sup>196</sup>H. Akimichi, T. Inoshita, S. Hotta, H. Noge, and H. Sakaki, “Structure of pentacene/tetracene superlattices deposited on glass substrate,” *Appl. Phys. Lett.* **63**, 3158–3160 (1993).
- <sup>197</sup>R. Kurihara, T. Hosokai, and Y. Kubozono, “Growth and structure of picene thin films on SiO<sub>2</sub>,” *Mol. Cryst. Liq. Cryst.* **580**, 83–87 (2013).
- <sup>198</sup>T. Hosokai, A. Hinderhofer, F. Bussolotti, K. Yonezawa, C. Lorch, A. Vorobiev, Y. Hasegawa, Y. Yamada, Y. Kubozono, A. Gerlach, S. Kera, F. Schreiber, and N. Ueno, “Thickness and substrate dependent thin film growth of picene and impact on the electronic structure,” *J. Phys. Chem. C* **119**, 29027–29037 (2015).
- <sup>199</sup>R. Hayakawa, A. Turak, X. Zhang, N. Hiroshiba, H. Dosch, T. Chikyow, and Y. Wakayama, “Strain-effect for controlled growth mode and well-ordered structure of quaterylene thin films,” *J. Chem. Phys.* **133**, 034706 (2010).

- <sup>200</sup>X. Zhang, E. Barrena, D. Goswami, D. G. de Oteyza, C. Weis, and H. Dosch, "Evidence for a layer-dependent Ehrlich-Schwöbel barrier in organic thin film growth," *Phys. Rev. Lett.* **103**, 136101 (2009).
- <sup>201</sup>T. Toccoli, P. Bettotti, A. Cassinese, S. Gottardi, Y. Kubozono, M. A. Loi, M. Manca, and R. Verucchi, "Photophysics of pentacene-doped picene thin films," *J. Phys. Chem. C* **122**, 16879–16886 (2018).
- <sup>202</sup>J.-O. Vogel, I. Salzmann, R. Opitz, S. Duhm, B. Nickel, J. P. Rabe, and N. Koch, "Sub-nanometer control of the interlayer spacing in thin films of intercalated rodlike conjugated molecules," *J. Phys. Chem. B* **111**, 14097–14101 (2007).
- <sup>203</sup>J. Lang, D. J. Sloop, and T.-S. Lin, "Dynamics of *p*-terphenyl crystals at the phase transition temperature: A zero-field EPR study of the photoexcited triplet state of pentacene in *p*-terphenyl crystals," *J. Phys. Chem. A* **111**, 4731–4736 (2007).
- <sup>204</sup>R. W. Olson and M. D. Fayer, "Site-dependent vibronic line widths and relaxation in the mixed molecular crystal pentacene in *p*-terphenyl," *J. Phys. Chem.* **84**, 2001–2004 (1980).
- <sup>205</sup>J. Köhler, A. Brouwer, E. Groenen, and J. Schmidt, "On the intersystem crossing of pentacene in *p*-terphenyl," *Chem. Phys. Lett.* **250**, 137–144 (1996).
- <sup>206</sup>W. P. Ambrose, T. Basché, and W. E. Moerner, "Detection and spectroscopy of single pentacene molecules in a *p*-terphenyl crystal by means of fluorescence excitation," *J. Chem. Phys.* **95**, 7150–7163 (1991).
- <sup>207</sup>H. de Vries and D. A. Wiersma, "Fluorescence transient and optical free induction decay spectroscopy of pentacene in mixed crystals at 2 K. Determination of intersystem crossing and internal conversion rates," *J. Chem. Phys.* **70**, 5807–5822 (1979).
- <sup>208</sup>W. H. Hesselink and D. A. Wiersma, "Vibronic relaxation in molecular mixed crystals: Pentacene in naphthalene and *p*-terphenyl," *J. Chem. Phys.* **74**, 886–889 (1981).
- <sup>209</sup>D. Lubert-Perquel, A. A. Szumska, M. Azzouzi, E. Salvadori, S. Ruloff, C. M. W. Kay, J. Nelson, and S. Heutz, "Structure dependence of kinetic and thermodynamic parameters in singlet fission processes," *J. Phys. Chem. Lett.* **11**, 9557–9565 (2020).
- <sup>210</sup>A. M. Alvertis, R. Pandya, L. A. Muscarella, N. Sawhney, M. Nguyen, B. Ehrler, A. Rao, R. H. Friend, A. W. Chin, and B. Monserrat, "Impact of exciton delocalization on exciton-vibration interactions in organic semiconductors," *Phys. Rev. B* **102**, 081122 (2020).
- <sup>211</sup>C.-C. Shen, W.-Y. Chou, and H.-L. Liu, "Temperature dependence of optical properties of pentacene thin films probed by spectroscopic ellipsometry," *Solid State Commun.* **188**, 1–4 (2014).
- <sup>212</sup>K. A. Kistler, C. M. Pochas, H. Yamagata, S. Matsika, and F. C. Spano, "Absorption, circular dichroism, and photoluminescence in perylene diimide bichromophores: Polarization-dependent H- and J-aggregate behavior," *J. Phys. Chem. B* **116**, 77–86 (2012).
- <sup>213</sup>P. Bounds, W. Siebrand, I. Eisenstein, R. Munn, and P. Petelenz, "Calculation and spectroscopic assignment of charge-transfer states in solid anthracene, tetracene and pentacene," *Chem. Phys.* **95**, 197–212 (1985).
- <sup>214</sup>K. Vandewal, J. Benduhn, K. S. Schellhammer, T. Vangerven, J. E. Rückert, F. Piersimoni, R. Scholz, O. Zeika, Y. Fan, S. Barlow, D. Neher, S. R. Marder, J. Manca, D. Spoltore, G. Cuniberti, and F. Ortman, "Absorption tails of donor:C<sub>60</sub> blends provide insight into thermally activated charge-transfer processes and polaron relaxation," *J. Am. Chem. Soc.* **139**, 1699–1704 (2017).
- <sup>215</sup>C. Zeiser, C. Cruz, D. R. Reichman, M. Seitz, J. Hagenlocher, E. L. Chronister, C. J. Bardeen, R. Tempelaar, and K. Broch, "Vacancy control in acene blends links exothermic singlet fission to coherence," *Nat. Commun.* **12**, 5149 (2021).
- <sup>216</sup>C. P. Theurer, A. M. Valencia, J. Hausch, C. Zeiser, V. Sivanesan, C. Cocchi, P. Tegeder, and K. Broch, "Photophysics of charge transfer complexes formed by tetracene and strong acceptors," *J. Phys. Chem. C* **125**, 6313–6323 (2021).
- <sup>217</sup>R. A. Street, D. Davies, P. P. Khlyabich, B. Burkhart, and B. C. Thompson, "Origin of the tunable open-circuit voltage in ternary blend bulk heterojunction organic solar cells," *J. Am. Chem. Soc.* **135**, 986–989 (2013).
- <sup>218</sup>Y. Zhen, H. Tanaka, K. Harano, S. Okada, Y. Matsuo, and E. Nakamura, "Organic solid solution composed of two structurally similar porphyrins for organic solar cells," *J. Am. Chem. Soc.* **137**, 2247–2252 (2015).